

**DEVELOPMENT OF STYRENE-BUTYL ACRYLATE-ISOPRENE  
EMULSION COPOLYMER COATING FOR NATURAL RUBBER  
GLOVES**

**CHAREEYA A/P I GI**

**FACULTY OF SCIENCE  
UNIVERSITI MALAYA  
KUALA LUMPUR**

**2022**

**DEVELOPMENT OF STYRENE-BUTYL ACRYLATE-ISOPRENE  
EMULSION COPOLYMER COATING FOR NATURAL RUBBER  
GLOVES**

**CHAREEYA A/P I GI**

**DISSERTATION SUBMITTED IN  
FULFILMENT OF THE  
REQUIREMENTS FOR THE DEGREE  
OF MASTER OF SCIENCE**

**DEPARTMENT OF CHEMISTRY  
FACULTY OF SCIENCE  
UNIVERSITI MALAYA  
KUALA LUMPUR**

**2022**

**UNIVERSITI MALAYA**  
**ORIGINAL LITERARY WORK DECLARATION**

Name of Candidate: **CHAREEYA A/P I GI**

Matric No: **17120655/2**

Name of Degree: **MASTER BY RESEARCH**

Title of Dissertation ("this Work"):

**DEVELOPMENT OF STYRENE-BUTYL ACRYLATE-ISOPRENE  
EMULSION COPOLYMER COATING FOR NATURAL RUBBER GLOVES**

Field of Study: **POLYMER CHEMISTRY**

I do solemnly and sincerely declare that:

- (1) I am the sole author/writer of this Work;
- (2) This Work is original;
- (3) Any use of any work in which copyright exists was done by way of fair dealing and for permitted purposes and any excerpt or extract from, or reference to or reproduction of any copyright work has been disclosed expressly and sufficiently and the title of the Work and its authorship have been acknowledged in this Work;
- (4) I do not have any actual knowledge nor do I ought reasonably to know that the making of this work constitutes an infringement of any copyright work;
- (5) I hereby assign all and every rights in the copyright to this Work to the University of Malaya ("UM"), who henceforth shall be owner of the copyright in this Work and that any reproduction or use in any form or by any means whatsoever is prohibited without the written consent of UM having been first had and obtained;
- (6) I am fully aware that if in the course of making this Work I have infringed any copyright whether intentionally or otherwise, I may be subject to legal action or any other action as may be determined by UM.

Candidate's Signature

Date: 28/12/2022

Subscribed and solemnly declared before,

Witness's Signature

Date: 28/12/2022

Name:

Designation:

# **DEVELOPMENT OF STYRENE-BUTYL ACRYLATE-ISOPRENE EMULSION COPOLYMER COATING FOR NATURAL RUBBER GLOVES**

## **ABSTRACT**

Coating natural rubber gloves with a layer of polymeric film is an essential process to improve donning properties of the gloves. In particular, polymeric coating with low coefficient of friction (CoF) is preferable for fast and easy donning. When coating an elastomeric article, there is an additional consideration where the coating layer can delaminate easily from the rubber substrate since the rubber article can be readily stretched. Hence, it is crucial to choose a right combination and composition of monomers to produce coating with a smooth surface and do not delaminate easily when stretched. In this research study, a newly developed styrene-butyl acrylate-isoprene (St-BA-Iso) emulsion copolymer was synthesized via seeded emulsion polymerization technique and the main objective of this study is to examine the effect of varying the composition of soft and hard monomers on the properties of emulsion and its coating performance in rubber gloves coating application. A series of St-BA-Iso emulsions of different monomers' weight ratio were synthesized, and were subsequently formulated into polymeric coating solution to be coated on natural rubber film. The copolymers were characterized spectroscopically, as well as via microscopy, thermal and physical analyses. Carefully designed methodology and formulation has allowed the emulsions synthesis to achieve  $\geq 90$  % conversion,  $41 \pm 2$  wt. % of total solid content, and desirable emulsions' stability. In terms of coating performance on natural rubber film, copolymers comprised of higher loadings of soft monomers BA and Iso produced sticky films with a comparatively low glass transition temperature and higher CoF. Conversely, high loading of hard monomer St in the copolymer produced smooth coating surface with lower CoF but resulted in significant delamination from the rubber substrate when stretched due to

high stiffness and poor coating adhesion. Of all synthesized copolymers, sample denoted as St-40 with 4 St: 3 BA: 3 Iso composition outperformed the rest as it was able to achieve a well-balanced donning properties, by demonstrating impressively smooth coating surface and at the same time retaining good coating adhesion on the rubber substrate. Hence, this makes St-40 an ideal copolymer emulsion for rubber glove coating applications.

**Keywords:** emulsion copolymer; natural rubber glove coating; styrene-butyl acrylate-isoprene; coefficient of friction; easy donning

Universiti Malaysia

# **PERKEMBANGAN SALUTAN EMULSI KOPOLIMER STIRENA-BUTIL AKRILAT-ISOPRENA UNTUK SARUNG TANGAN GETAH ASLI**

## **ABSTRAK**

Penyalutan sarung tangan getah asli dengan lapisan filem polimer merupakan satu proses penting untuk memperbaiki ciri-ciri sarung tangan getah. Khususnya, salutan polimer dengan pekali geseran (CoF) yang rendah adalah lebih baik untuk sarungan yang cepat dan mudah. Semasa menyalut artikel elastomerik, pertimbangan perlu diambil kira di mana lapisan salutan boleh tertanggal dengan mudah dari permukaan getah kerana artikel getah mudah diregang. Oleh hal yang demikian, adalah penting untuk memilih kombinasi dan komposisi monomer yang sesuai untuk menghasilkan salutan yang dapat melicinkan permukaan sarung tangan dan tidak mudah tertanggal apabila sarung tangan tersebut diregangkan. Dalam kajian penyelidikan ini, emulsi stirena-butil akrilat-isoprena (St-BA-Iso) telah disintesis melalui teknik pempolimeran emulsi benih dan objektif utama kajian ini adalah untuk mengkaji kesan-kesan perubahan komposisi monomer lembut dan monomer keras ke atas sifat emulsi dan prestasi salutannya dalam aplikasi salutan sarung tangan getah. Satu siri emulsi St-BA-Iso telah disintesis menggunakan nisbah berat monomer yang berbeza, dan kemudiannya diformulasikan menjadi larutan polimer untuk disalutkan pada filem getah asli. Ciri-ciri kopolimer tersebut telah dikaji melalui ujian spektroskopi, mikroskopi, haba dan analisa fizikal. Metodologi dan formulasi yang direka dengan teliti telah membolehkan sintesis emulsi mencapai penukaran monomer sebanyak  $\geq 90\%$ ,  $41 \pm 2$  wt% jumlah kandungan pepejal, dan kestabilan emulsi yang diinginkan. Dari segi prestasi salutan pada filem getah asli, kopolimer yang mempunyai komposisi monomer lembut yang lebih banyak iaitu butil akrilat dan isoprena menghasilkan filem yang melekit dengan suhu peralihan kaca yang agak rendah dan CoF yang lebih tinggi. Sebaliknya, komposisi monomer keras St yang lebih banyak dalam kopolimer

menghasilkan permukaan salutan yang licin dengan CoF yang lebih rendah, namun demikian salutan tersebut mudah tertanggal dari permukaan getah apabila diregangkan disebabkan oleh tahap kekejuran yang tinggi dan lekatan salutan yang lemah. Antara semua kopolimer yang disintesis, sampel dengan notasi St-40 dengan nisbah berat 4 St: 3 BA: 3 Iso telah mengungguli kopolimer lain kerana ia dapat mencapai sifat sarung yang seimbang dengan mempamerkan permukaan salutan yang licin dan pada masa yang sama dapat mengekalkan lekatan salutan yang baik pada permukaan getah. Oleh yang demikian, ini telah menjadikan St-40 emulsi kopolimer yang ideal untuk aplikasi salutan sarung tangan getah.

**Kata kunci:** emulsi kopolimer; salutan sarung tangan getah asli; stirena-butil akrilat-isoprena; pekali geseran; mudah sarung

## ACKNOWLEDGEMENTS

The research and development of emulsion copolymer coating for natural rubber glove application is a cooperative effort and contributions of several individuals and organizations. First and foremost, I would like to convey my heartfelt gratitude to my supervisor Dr. Desmond Ang Teck Chye and Professor Dr. Gan Seng Neon, for their guidance, dedication, supervision and unparalleled expertise for the continuous support of my Master's research work. Their guidance has helped me throughout the research journey, paper publication and writing of this dissertation. I am grateful to be working with them and could not have imagined having better supervisor to complete my Master's project.

My sincere thanks also goes to Ms. Adeline Ling, Mr. Low Meng Lai, Mr. Shahrul and in particular, Mr. Chiam Han Cheng from Top Glove International Sdn. Bhd. for their full assistance and guidance, insightful knowledge and comments, especially in guiding me with lab works related to industry. Also, thank you for their valuable technical advices and helpful discussions throughout this study and keeping updated on my progress from the beginning until the end of the project. The appreciation also goes to my fellow colleagues and staffs from Top Glove International Sdn. Bhd. who have helped me directly and indirectly during my time training there.

On top of that, it has also been a pleasure to work with my fellow lab mates and postgraduate students: Yong Ming Yee, Natasya Nabilla, Assiela Aiman, Deepa, Tan Tiek Aun and Nik Humaidi for sharing their knowledge as well as keep on motivating and encouraging me in a positive way throughout my Master's journey. Without them as my happy pill, I could not carry on the project with full passion and enthusiasm.



I am also truly grateful for the funding for this work which has been provided by Public-Private Research Network [PV066-2019], in collaboration with private funding from a renowned rubber gloves company Top Glove Sdn. Bhd. [PV007-2020]. With these funding, this research study has been carried out and completed successfully.

My deepest appreciation also goes to both of my parents Mr. I Gi and Mdm. Ratna for their love, prayers, moral supports and sacrifices for educating me and shaping me to become who I am today. Last but not least, I would also like to extend my appreciation to the lab assistants and supporting staffs for their assistance as well as the Department of Chemistry, Faculty of Science and Universiti Malaya for providing the facilities and services to complete my Master's study.

## TABLE OF CONTENT

<b>ABSTRACT .....</b>	<b>iii</b>
<b>ABSTRAK .....</b>	<b>v</b>
<b>ACKNOWLEDGEMENTS.....</b>	<b>vii</b>
<b>TABLE OF CONTENT.....</b>	<b>ix</b>
<b>LIST OF FIGURES .....</b>	<b>xiii</b>
<b>LIST OF TABLES .....</b>	<b>xv</b>
<b>LIST OF SYMBOLS AND ABBREVIATIONS .....</b>	<b>xvi</b>
<b>LIST OF APPENDICES .....</b>	<b>xix</b>
<b>CHAPTER 1 : INTRODUCTION.....</b>	<b>1</b>
1.1 Background.....	1
1.2 Objectives of study .....	3
1.3 Dissertation outline.....	4
<b>CHAPTER 2 : LITERATURE REVIEW.....</b>	<b>5</b>
2.1 Origin of emulsion polymerization.....	5
2.2 Components of emulsion polymerization.....	6
2.2.1 Continuous medium .....	7
2.2.2 Surfactants.....	7
2.2.3 Monomer.....	9
2.2.4 Initiator.....	11
2.3 Mechanism of emulsion polymerization .....	12
2.3.1 Stage I (Particle nucleation).....	12

2.3.2	Stage II (Particle growth) .....	14
2.3.3	Stage III (Monomer finishing) .....	14
2.4	In-situ seeded emulsion polymerization technique.....	15
2.5	Glove coating application .....	17
2.5.1	Origin of glove .....	17
2.6	Types of gloves coating .....	18
2.6.1	Powdered gloves .....	18
2.6.2	Chlorination .....	19
2.6.3	Polymeric coating.....	20
2.7	Properties of polymer coating on rubber films .....	22
2.7.1	Surface smoothness .....	22
2.7.2	Film flexibility and surface adhesion .....	23
2.8	Film formation mechanism.....	24
<b>CHAPTER 3 : EXPERIMENTAL .....</b>		<b>26</b>
3.1	Materials .....	26
3.2	Apparatus .....	26
3.3	Synthesis of St-BA-Iso emulsion.....	27
3.4	Characterization of St-BA-Iso emulsion .....	30
3.4.1	Extent of conversion and total solid content (TSC).....	30
3.4.2	pH value .....	30
3.4.3	Surface tension .....	30
3.4.4	Particle size .....	31

3.4.5	Zeta potential.....	31
3.5	Characterization of St-BA-Iso copolymer.....	32
3.5.1	Attenuated total reflectance – Fourier transform infrared (ATR-FTIR)...	32
3.5.2	Proton Nuclear Magnetic Resonance ( $^1\text{H}$ -NMR).....	33
3.5.3	Gel Permeation Chromatography (GPC) .....	34
3.5.4	Thermogravimetric Analysis (TGA).....	35
3.5.5	Differential Scanning Calorimetry (DSC) .....	36
3.5.6	Tensile test .....	37
3.6	Polymer coating on rubber film.....	38
3.6.1	Compounding of St-BA-Iso polymer coating solution .....	38
3.6.2	Preparation of rubber film coated with St-BA-Iso copolymer.....	39
3.7	Properties of coated rubber film .....	41
3.7.1	Coefficient of friction (CoF) .....	41
3.7.2	Physical tests and visual inspections.....	42
3.7.3	Scanning Electron Microscope (SEM).....	43
<b>CHAPTER 4 : RESULTS AND DISCUSSION .....</b>		<b>44</b>
4.1	Characterization of St-BA-Iso emulsion .....	44
4.1.1	Extent of conversion and TSC %.....	44
4.1.2	Physical properties .....	45
4.2	Characterization of St-BA-Iso copolymer film .....	51
4.2.1	ATR-FTIR.....	51
4.2.2	$^1\text{H}$ -NMR .....	54

4.2.3	TGA .....	56
4.2.4	DSC .....	58
4.2.5	Tensile test .....	60
4.3	Coating performance on rubber substrate .....	62
4.3.1	Coefficient of friction .....	63
4.3.2	Visual evaluation on polymer coated rubber film .....	64
4.3.3	SEM analysis .....	66
<b>CHAPTER 5 : CONCLUSION .....</b>		<b>69</b>
5.1	Summary .....	69
5.2	Suggestions for future work .....	70
<b>REFERENCES .....</b>		<b>72</b>
<b>APPENDIX .....</b>		<b>81</b>

## LIST OF FIGURES

Figure 2.1	: General classification of surfactant .....	8
Figure 2.2	: Three main stages in emulsion polymerization.....	15
Figure 2.3	: General process manufacture flow of polymer-coated rubber gloves in industry.....	22
Figure 2.4	: Three main stages involved in film formation mechanism.....	25
Figure 3.1	: Experimental set-up for emulsion polymerization.....	27
Figure 3.2	: Proposed structure of St-BA-Iso copolymer.....	29
Figure 3.3	: Particle size analyser Horiba LA960A.....	31
Figure 3.4	: Zetasizer Malvern Nano ZS.....	32
Figure 3.5	: Perkin Elmer ATR-FTIR spectrum 400 spectrometer.....	33
Figure 3.6	: JEOL 400 MHz resonance spectrometer.....	34
Figure 3.7	: GPC Waters e2695.....	35
Figure 3.8	: Perkin Elmer TGA-4000.....	36
Figure 3.9	: TA Instruments DSC Q20.....	37
Figure 3.10	: Universal testing machine Sirius Hexa-6.....	38
Figure 3.11	: 2% TSC polymer coating solution.....	39
Figure 3.12	: Illustration of dipping process involved.....	40
Figure 3.13	: Lab-scale dipping setup.....	41
Figure 3.14	: Leading Instruments COF-02.....	41
Figure 3.15	: 'X' mark for water turbidity test.....	43
Figure 3.16	: (a) JEOL JSM-6010LV SEM sample chamber, (b) JEOL gold coater.....	43
Figure 4.1	: Particle size distribution curves of synthesized emulsions.....	47
Figure 4.2	: Detailed particle size curves for each emulsion.....	47
Figure 4.3	: Zeta potential distribution curves of all emulsions.....	49
Figure 4.4	: Zeta potential distribution curve for St-60.....	49

Figure 4.5	: Zeta potential distribution curve of St-40.....	50
Figure 4.6	: Zeta potential distribution curve of BA-60.....	50
Figure 4.7	: Zeta potential distribution curve of BA-40.....	50
Figure 4.8	: Zeta potential distribution curve of Iso-60.....	51
Figure 4.9	: Zeta potential distribution curve of Iso-40.....	51
Figure 4.10	: FTIR spectra of St, BA, and Iso monomers.....	53
Figure 4.11	: FTIR spectra of (a) St-60, (b) St-40, (c) BA-60, (d) BA-40, (e) Iso-60, (f) Iso-40 copolymers.....	53
Figure 4.12	: <sup>1</sup> H-NMR spectrum of the St-40 copolymer.....	55
Figure 4.13	: TGA thermograms of St-BA-Iso copolymers.....	57
Figure 4.14	: First derivative TGA thermograms of St-BA-Iso copolymers.....	58
Figure 4.15	: DSC thermograms of St-BA-Iso terpolymer films.....	60
Figure 4.16	: Force-displacement curves of St-BA-Iso copolymer films.....	62
Figure 4.17	: (a) White patch appearance of films after stretched and (b) water cloudiness from water turbidity test.....	66
Figure 4.18	: Stretched rubber films coated with St-BA-Iso copolymer.....	68

## LIST OF TABLES

Table 3.1	: Literature value of monomers' properties .....	27
Table 3.2	: Monomer compositions of a series of St-BA-Iso emulsion copolymer.....	28
Table 3.3	: Detailed formulation on the synthesis of St-BA-Iso emulsion copolymers.....	28
Table 3.4	: Compounding formulation.....	39
Table 4.1	: Conversion and TSC % of St-BA-Iso emulsions.....	45
Table 4.2	: Physical properties of St-BA-Iso emulsions.....	46
Table 4.3	: Assignment of characteristic IR peaks for each monomers.....	54
Table 4.4	: Assignment of characteristic IR peaks for St-BA-Iso copolymers..	54
Table 4.5	: Attribution and chemical shifts of St-40 from <sup>1</sup> H-NMR analysis...	56
Table 4.6	: Glass transition temperature (T <sub>g</sub> ) of St-BA-Iso terpolymer films...	59
Table 4.7	: Mechanical test outcomes for St-BA-Iso copolymers.....	61
Table 4.8	: T <sub>g</sub> of homopolymers and its functions.....	62
Table 4.9	: Kinetic CoF values for uncoated rubber films and rubber films coated with St-BA-Iso copolymers.....	64
Table 4.10	: Film tackiness inspection and outcomes from blocking test.....	65



## LIST OF SYMBOLS AND ABBREVIATIONS

%	:	Percentage
$\bar{x}$	:	Mean
°C	:	Degree Celsius
$\delta$	:	Chemical shift
$\mu\text{m}$	:	Micrometre
$^1\text{H-NMR}$	:	Proton Nuclear Magnetic Resonance
AA	:	Acrylic acid
ASTM D189-14	:	Standard Test Method for Static and Kinetic Coefficients of Friction of Plastic Film and Sheeting
ATR-FTIR	:	Attenuated total reflectance – Fourier transform infrared
BA-40	:	Copolymer with 30 St: 40 BA: 30 Iso monomer ratio
BA-60	:	Copolymer with 20 St: 60 BA: 20 Iso monomer ratio
$\text{CDCl}_3$	:	Deuterated chloroform
cm	:	Centimetre
CMC	:	Critical micelle concentration
CoF	:	Coefficient of friction
DSC	:	Differential Scanning Calorimetry
EN455-2	:	Medical gloves for single use – Part 2: Requirements and testing for physical properties
g/mL	:	Gram per millilitre
g/mol	:	Gram per mole
GPC	:	Gel permeation chromatography
h	:	Hours
Iso-40	:	Copolymer with 30 St: 30 BA: 40 Iso monomer ratio
Iso-60	:	Copolymer with 20 St: 20 BA: 60 Iso monomer ratio
KPS	:	Potassium persulfate

L	:	Litre
MFFT	:	Minimum film forming temperature
MHz	:	Megahertz
min	:	Minutes
MPa	:	Megapascal
mg	:	Milligram
mV	:	Millivolt
$M_v$	:	Molecular weight
N/m	:	Newton per meter
$\text{Na}_2\text{S}_2\text{O}_4$	:	Sodium dithionite
NaOH	:	Sodium hydroxide
NBR	:	Nitrile butadiene rubber
$\text{NH}_3$ aq.	:	Aqueous ammonia
nm	:	Nanometre
NR	:	Natural rubber
ppm	:	Part per million
PTFE	:	Polytetrafluoroethylene
R&D	:	Research & Development
rpm	:	Rotation per minute
s	:	Seconds
SDBS	:	Sodium Dodecyl Benzene Sulfonate
SEM	:	Scanning Electron Microscopy
St-40	:	Copolymer with 40 St: 30 BA: 30 Iso monomer ratio
St-60	:	Copolymer with 60 St: 20 BA: 20 Iso monomer ratio
St-BA-Iso	:	Styrene-butyl acrylate-isoprene
$T_g$	:	Glass transition temperature

TGA	:	Thermogravimetric analysis
THF	:	Tetrahydrofuran
T <sub>p</sub>	:	Maximum rate of weight loss
TSC	:	Total solid content
VOCs	:	Volatile organic compounds
w/v %	:	Percentage of weight over volume
wt. %	:	Weight percentage %

Universiti Malaya

## LIST OF APPENDICES

Appendix A : DSC thermogram of St-60.....	81
Appendix B : DSC thermogram of St-40.....	82
Appendix C : DSC thermogram of BA-60.....	82
Appendix D : DSC thermogram of BA-40 .....	83
Appendix E : DSC thermogram of Iso-60.....	83
Appendix F : DSC thermogram of Iso-40.....	84

## CHAPTER 1 : INTRODUCTION

### 1.1 Background

Rubber gloves are primarily used in fields such as medical, industrial, food handling, and housekeeping to protect wearers' hands against infection, diseases, chemicals, or static electricity. Natural rubber gloves and synthetic nitrile rubber gloves account for the vast majority of the mentioned applications due to their versatility and affordable cost. Nevertheless, tightly fitting gloves fabricated from elastomeric materials such as natural rubber latex often suffered from donning difficulty due to its inherent high coefficient of friction. Though the primary function of glove is to protect human hands from hazardous environmental factors, the ease of donning and comfort while wearing them also plays a significant role.

Conventional gloves are typically covered with a layer of powdered lubricant on the gloves' inner surface to ease donning. Most commonly, powder such as talc or corn-starch is dusted onto the inner surface of the glove during manufacturing. While the use of powder does make the glove donning easier, it is not suitable for all applications. For example, the loose dusting powder on surgical gloves might dislodge from the gloves and inadvertently enters the surgical site, contaminating the wound and causes post-operative complications to the patient. Alternatively, latex gloves may be chlorinated with dilute chlorine solution to harden the product surface which may bring ease in donning. However, some of the drawbacks of chlorination is deterioration in physical properties of the chlorinated gloves on thermal ageing, presence of strong odor, possible skin irritation, and discoloration.

A better alternative is the application of a layer of polymer coating onto the glove surface to reduce the surface tackiness. Wide variety of polymers which exhibited low surface tack property have been used for this purpose and the most recent ones include

carboxylated styrene-butadiene (SBR); anionic polyurethane and styrene-acrylic based resins. However, the production of SBR is a great challenge and inconvenience to many as it involves hazardous butadiene monomer which is highly flammable and can easily trigger explosion without proper handling during its operation (Sun & Wristers, 2000). As for polyurethane, the synthesis involves potentially carcinogenic and toxic monomer known as isocyanate, and the gloves coated with polyurethane also often suffers from exfoliation problem (Kieć-Świerczyńska et al., 2014).

Although several types of polymer coatings have been reported in recent years, most are lab-scale innovations which are rather expensive, making them less appealing to the industry. Besides, some only exhibit average performance in reducing the coefficient of friction of rubber film. In addition to that, there has not been much new innovations on the type of copolymer coatings for rubber glove application. Most of these resins developed are either homopolymer or simple copolymer which utilize only one or two monomers, limiting formulation flexibility and make it difficult to attain certain required film properties. Instead, with advances in this study focusing on the optimal combination of 3 different monomers to produce a copolymer, the property of coating film can be easily tuned and improved by tailoring the ratio of monomers used, as well as selecting the right monomer combination for the synthesis (Hua & Dubé, 2011; Jiao et al., 2021).

In view of the above-mentioned limitations, the objective of this research is to develop a novel emulsion copolymer which is relatively safe, involves simpler setup, and uses less-toxic chemicals. A new combination of styrene-butyl acrylate-isoprene (St-BA-Iso) copolymer developed in this work able to produce coating with excellent film properties and suitable for rubber glove application. Hard monomer styrene was selected as one of the monomers for synthesis as it can enhance the surface hardness and contribute to the formation of smoother film surface. On the other hand, the soft monomers butyl acrylate

and isoprene were included in the formulation to derive excellent flexibility and adhesion property (Zhong et al., 2013). In addition, the diene monomer used in this formulation, isoprene is relatively safe and industrial-friendly compared to the butadiene gas used for the synthesis of conventional SBR.

In this work, St-BA-Iso emulsion was prepared via semi-continuous emulsion polymerization technique, and subsequently formulated as polymeric coating to be applied on the donning side of natural rubber article. Apart from that, it is also crucial to employ a reasonable combination of hard and soft monomers to ensure that the polymer coating can achieve the desired film properties. Thus, this study also provides an insight on the effect of manipulating the ratio of hard to soft monomers in the novel St-BA-Iso copolymer emulsion for rubber gloves coating application. By varying the ratio of hard to soft monomer, the  $T_g$  of the film will change, rendering the film properties to alter evidently. The physical properties of the synthesized St-BA-Iso emulsion and its coating performance were characterized and compared with the commercial SBR and PU resins for benchmarking and comparison purpose.

## **1.2 Objectives of study**

The key feature to improve donning properties of rubber gloves is to reduce tackiness of the rubber surface, or by decreasing its coefficient of friction (CoF). Thus, the aim of this research project is to produce natural rubber latex glove with improved donning property (low CoF) by applying a layer of novel copolymer. To achieve the aim, following specific objectives were drawn out:

- i. To synthesize and characterize emulsion copolymer of styrene-butyl acrylate-isoprene (St-BA-Iso) of varied composition for rubber glove coating application.

- ii. To compound and coat St-BA-Iso copolymers on natural rubber latex film.
- iii. To characterize the properties of the natural rubber latex film coated with St-BA-Iso copolymers.

### **1.3 Dissertation outline**

This dissertation comprised of five chapters. First and foremost, Chapter 1 provides a brief introduction on the background and objectives of the study. Next, Chapter 2 presents a review on literatures related to the subject of this study. Chapter 3 covered experimental chemicals and procedures involved in the synthesis of St-BA-Iso emulsions, compounding, as well as the coating procedure. Methodology and instrumental techniques used to analyse the emulsions, and the properties of the coated rubber films were reported in this chapter too. Chapter 4 presents the results obtained in this study, comprising of the properties of the synthesized St-BA-Iso emulsions, as well as the copolymers film properties and their coating performance on rubber substrate. Lastly, in Chapter 5, conclusions and future work were elaborated.



## CHAPTER 2 : LITERATURE REVIEW

### 2.1 Origin of emulsion polymerization

Emulsion polymerization is an important industrial process that is widely used to produce a great variety of polymers for various applications such as binders, paints, adhesives, coatings, varnishes, etc. (Paulen et al., 2013). An emulsion consists of a discontinuous liquid phase dispersed in a separate, continuous liquid phase. Examples of emulsions that occur naturally are milk and the sap of the rubber tree (*Hevea brasiliensis*). During World War II, there was exponential increase in demand for natural rubber, and this has eventually led to shortage of natural rubber supply. Consequently, 1,3-butadiene and styrene was used to produce synthetic rubber, making it the first emulsion polymer ever produced (Lovell & Schork, 2020). Since then, development of synthetic rubber by emulsion polymerization has grown considerably and has also led to production of extremely wide range of polymers from various monomers.

Some examples of monomers that can be polymerized via emulsion polymerization are styrene, acrylates, methacrylates, chloroprene and vinyl acetate (Feldman, 2008). The final product from the emulsion polymerization process is referred to as “latex”. By analogy, latex is used to describe a colloidal dispersion of polymer particles in water, where it is stabilized by a colloid stabilizer known as surfactant. Latexes generally consist of 20-70 wt.% solids and the diameter of particles are within the range 50-1000 nm (Oadian, 2004). Typically, each particle is made up of 1-10000 polymer chains, and each polymer chain consisted of  $10^2$ - $10^6$  monomeric units. Latex can be used without further separation. In industry, there are a vast range of products manufactured using latex, such as rubbers, paint, polishes, sealants, adhesives, plastics and paper coatings (Yamak, 2013).

One of the main reasons which has led to an extensive use of emulsion polymerization in various industries include the low viscosity of the latex at high polymer concentrations,

easy thermal control of the reaction mixture, the flexibility in controlling submicron particle size and morphology, the convenience of polymer separation from the latex or, in the case of coating applications, the final latex may be used directly (Lovell & Schork, 2020; Pladis & Kiparissides, 2014). In addition, another significant feature of emulsion polymerization is its capability to achieve higher polymerization rates and generate polymers of higher molecular weight when compared to other free-radical polymerization techniques.

Another significant advantage of the process is that there are almost no waste materials associated with the production of aqueous emulsions since all ingredients used throughout the process are retained in the end product. The only wastes are some filtration residues and monomer-contaminated process water such as pumps. Additionally, process emissions are relatively minimal because at most of the time, residual monomer stays in the final product (Lutz et al., 2012). Notwithstanding, over the last few decades, increasing awareness of environmental protection and growing environmental legislation on the control of volatile organic compounds (VOCs) emission has resulted in a massive development of emulsion polymers for water-borne coating applications, serving as the alternative to replace the traditional solvent-borne coatings (Jiao et al., 2021).

## **2.2 Components of emulsion polymerization**

Different ingredients are used in different latex formulations, but there are some key components present in every emulsion polymerization system such as water, surfactants, monomer(s) and initiator (El-hoshoudy, 2018). In addition, post-synthesis components such as biocides are often introduced as well to perform a specific function (Danková et al., 2020). Besides, the type and scale of synthesis also influence the number of ingredients to be included in the formulation. For instance, a laboratory scale R&D work often involves recipe which requires fewer ingredients as compared to a more complex

industrial scale emulsion polymerization that produces final product for the market. Nevertheless, ingredients added can influence polymerization rate of latex particles, as well as the final product's composition and properties.

### **2.2.1 Continuous medium**

In an emulsion polymerization, water acts as the continuous medium. This is because water has excellent ability to conduct heat, which increases the rate of polymerization while maintaining the reaction viscosity as close as water to prevent auto-acceleration (Lovell & Schork, 2020). Depending on the source, water hardness can vary and may affect size of particle, nucleation, as well as the stability of particle (Bassett & Hamielec, 1981). Hence, deionized water is often used for the synthesis. Apart from that, the water must have low content of oxygen. This is because oxygen is a free-radical scavenger that cause inhibition period and retard the reaction rate (Liao et al., 2001). Oxygen-free condition is important during emulsion polymerization reactions to avoid the inhibition effect of oxygen on the free-radical mechanism of polymerization (Van Herk & Gilbert, 2013). Therefore, prior to polymerization, water is typically purged with nitrogen gas to reduce the oxygen content in water.

### **2.2.2 Surfactants**

Surfactants, also known as surface active agents or emulsifiers are compounds that reduce the surface tension of a liquid (Asua, 2004). It is one of the important components in emulsion polymerization due to several reasons. Firstly, they stabilize the monomer droplets. Besides, they can generate micelles that can act as nucleation sites, and also helps in solubilizing the monomers and latex polymers. In addition, surfactants can prevent lump formation by stabilizing the growing polymer particles, forming a stable final product (Lovell & Schork, 2020; Tauer, 2020). Depending on the intended use of

the latex, the selection of surfactant in an emulsion is decisive as it can influence the number and particle size, stability, mechanical strength and the final latex properties.

Surfactants are classified into four categories according to the nature of hydrophilic segment: anionic, cationic, amphoteric and non-ionic (Levison, 2009) as shown in Figure 2.1. Among all, anionic surfactants with a long hydrophobic alkyl chain and a sulfate or sulfonate charged hydrophilic end group is most used due to their higher compatibility with negatively charge latex particles. Typical anionic surfactants include sodium dodecyl sulfonate, sodium dodecyl benzenesulfonate, and sodium dialkylsulfosuccinate (Gong et al., 2020; Lin et al., 2011; Pedro & Walters, 2019). Meanwhile, cationic surfactants are rarely used due to their incompatibility with latex particles, and one such example is trimethylalkylammonium chlorides (Sari et al., 2017). Amphoteric surfactants show anionic properties at higher pH; cationic properties at lower pH, examples include amine oxides and imidazoline carboxylates (Sarkar et al., 2021). Non-ionic surfactants are often used in conjunction with ionic surfactants, where the hydrophilic segment is a non-ionic component such as a polyol or a block of ethylene oxide polymer chain (Kamal et al., 2017).

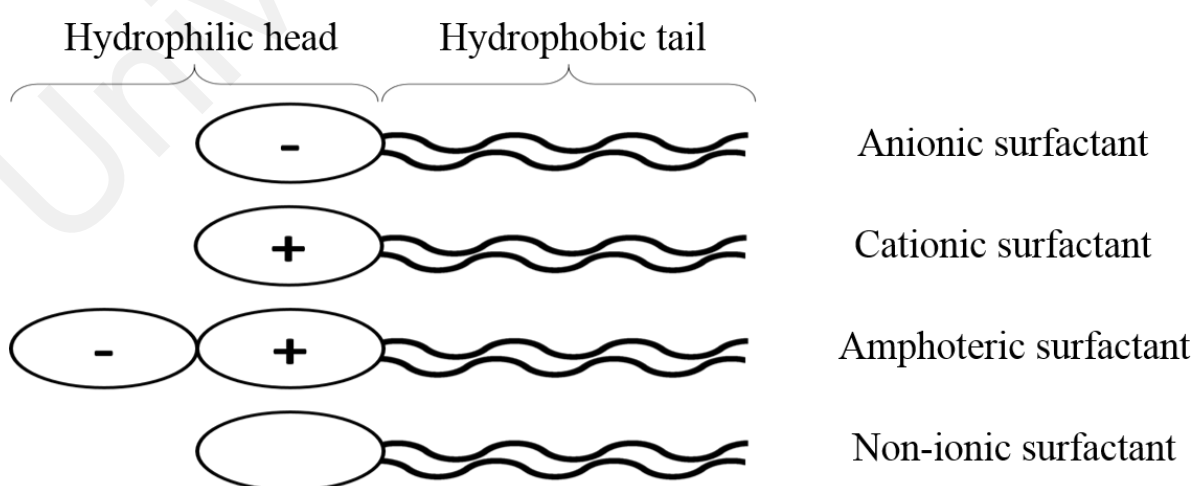


**Figure 2.1: General classification of surfactant**

Surfactant is composed of hydrophilic head and hydrophobic tail. Thus, owing to its amphiphilic property, surfactants tend to align themselves at interfaces of monomer droplets (Ren et al., 2019). Surfactants with high water solubility will be mainly found in the aqueous phase, while those of lower solubility can be found in the monomer droplets. At low concentration, surfactant molecules dissolve according to their solubility, but when the solution reaches a saturation point at critical micelle concentration (CMC), aggregation of surfactant molecules takes place to form small aggregates called “micelle” with a diameter range of 5-100 nm (Milovanovic et al., 2017). The hydrophobic ends of surfactant face inwards and the hydrophilic ends face outwards, forming a hydrophobic pocket (Cui et al., 2008). Since polar heads have like charges, micelles repel each other in water. The number and size of micelles formed depend on both the amount and nature of the surfactant. For example, smaller amounts of surfactant tend to result with bigger size micelles. Mostly, micelles have spherical shape, but they may appear rod-like too depending on the type and concentration of surfactant used (Asua, 2004; Van Herk & Gilbert, 2013).

### **2.2.3 Monomer**

Monomers are the building blocks of polymer chains in the latex particles. In emulsion polymerization, monomers constitute the oil phase. Styrene and other unsaturated hydrocarbon compounds are examples of monomers that are commonly polymerized via emulsion polymerization. Functional monomers like acrylic acid and methacrylic acid are also commonly added into the reaction in order to stabilize the emulsion, enhance adhesion, modify solubility of the polymer, as well as providing cross-linking sites (Kumar, 2017; Lesage de la Haye et al., 2017). Generally, monomers are insoluble in water, thus over 95 % of monomer molecules are found in monomer droplets suspended in water medium. The droplets having diameter range of 1-100 microns are stabilized by

surfactant molecules adsorbed onto the monomer droplets interface (Askari et al., 1993). Monomers may be in the hydrophobic pocket of the micelles or in the water. Highly soluble monomers may not form latex particles and may end up undergoing solution polymerization in water as the solvent (Jain et al., 2003).

There are a few considerations when it comes to selecting a monomer or its combination. This is because the monomers selected serve specific function and will determine the basic chemical, physical and thermal properties of the latex and the polymer produced. For example, desired glass transition temperature,  $T_g$  of the polymer product is significantly affected by the choice of monomers used. The  $T_g$  of a polymer is the temperature at which the polymer changes its property from a hard, brittle, and glassy state to a soft, flexible and rubbery state (Gong et al., 2018). To produce continuous films, target  $T_g$  of the polymer particle must be sufficiently low to enable sufficient polymer mobility for the interdiffusion of particle chains during film formation. Furthermore, concentration and chemical composition of monomer used will also influence the level of stiffness and strength of the polymer film produced from the latex (Wichaita et al., 2021).

Desired latex properties are hardly accomplished with the use of a single monomer. Instead, a combination of few monomers are usually needed to produce a copolymer with the desired properties (Wang et al., 2021). Formulation which comprises monomers that are known to produce glassy homopolymers will contribute to hardness, strength and clarity of the copolymer. On the other hand, soft monomers that usually produce rubbery homopolymers could contribute to better flexibility and adhesion of the copolymer. A combination of both hard and soft monomers may be necessary in certain applications.

Besides, consideration must also be given to the compatibility and stability of the latex particles. For instance, the particles in a latex that is to be employed in a paint formulation

should have good compatibility with the other coating components such as the fillers and pigments (Nishida et al., 1981). These properties may be affected by the presence of specific functional groups in the monomer. To improve colloidal stability, carboxyl functional monomers such as acrylic and methacrylic acids are frequently introduced in minimal dosage (usually 1-3 wt. %) (Yew et al., 2019). Other examples of functional monomers that can be included in the formulation are those with sulfonate, sulfate or hydroxyl groups. Besides, certain functionality in the monomers allow the polymers to crosslink covalently or ionically to improve its mechanical strength and film adhesion (Tan et al., 2016).

#### **2.2.4 Initiator**

In emulsion polymerization, initiators used are usually water soluble. The role of initiator is to yield free radicals, and they are usually produced via thermal decomposition, redox reactions, or by gamma radiation. The technique selected to produce free-radicals depends on the type of latex being synthesized and thus the temperature of the reaction. For instance, to prevent auto acceleration, initiators that generate radicals via redox reactions is used when synthesizing latex of high molecular weight at lower temperature (Van Herk & Gilbert, 2013). It consists of an oxidizing and reducing compound. The interaction between these components and optionally some multivalent metal ions generate radicals even at low temperature and allow smooth polymerization (Van Herk & Gilbert, 2013). Examples of redox initiator systems are based on iron (II) and peroxides, as well as peroxodisulfate-bisulfite.

In contrast, unlike redox initiators, thermal initiators are bound by temperature and activated by thermal energy as they do not release a sufficient amount of free-radicals at temperature lower than 50 °C. Typical polymerization temperatures are in the range of 70 – 90 °C (Lutz et al., 2012). Thermal initiators include peroxydisulfate salts such as

potassium persulfate and ammonium persulfate that decompose homolytically to generate sulfate radical anions (Asua, 2004; Bassett & Hamielec, 1981).

## **2.3 Mechanism of emulsion polymerization**

The mechanism by which emulsion polymers are synthesized is distinctly different in different system. The solubility of the monomers, surfactants and initiator in aqueous medium plays significant role in determining the polymerization mechanism. Emulsion polymerization is divided into three distinct stages (refer Figure 2.2) following the decomposition of the initiator: stage I (particle nucleation), stage II (particle growth), and stage III (monomer finishing) (Asua, 2004; Bassett & Hamielec, 1981; Van Herk & Gilbert, 2013).

### **2.3.1 Stage I (Particle nucleation)**

There are three principal mechanisms for particle nucleation, listed in order of when they were first discovered: (i) micellar nucleation, (ii) homogeneous nucleation, and (iii) droplet nucleation. There is possibility whereby all three mentioned mechanisms to run in parallel in an emulsion polymerization, however one is more likely to be dominant depending on the monomer, formulation of reaction, and reaction conditions.

Micellular nucleation or also known as heterogeneous nucleation has become one of the earliest suggested mechanism by Harkins (Harkins, 1945) whereby nucleation happens primarily in micelles and polymer particles. When the oil-insoluble initiator radical migrates into micelle which is filled with monomer molecules or also referred as monomer-swollen micelles, micellular nucleation starts. These radicals react within the micelle to form a monomer radical or an actively growing latex particle with a monomer (Erlangung & Nazaran, 2008). As Stage I progresses, the number of monomer-swollen micelles decreases and the number of particle nuclei increases, gradually lowering the



chance of an oligomeric radical to enter the monomer-swollen micelles. When all of the monomer-swollen micelles are eventually consumed, it marks the end of micellar nucleation (Lovell & Schork, 2020).

Over time, industrial professionals have widely recognized homogeneous nucleation, which is the second theory of nucleation and has become the primary form of nucleation. In this mechanism, when radicals released from the initiator in the aqueous medium react with the monomer molecules in the aqueous medium, it initiates polymerization to occur, which differentiates this from the first theory where polymerization occurs in the micelles. Consecutively, few more monomers will be added onto this radical, forming a polymer chain until it exceeds a threshold length in which the oligomer is hardly soluble in water. At this point, the chain is thermodynamically unstable. Thus, it will either collapse on itself or onto dead oligomers present in the aqueous medium to yield latex particles. At the same time, surfactant molecules adsorb onto their surface to stabilize the growing latex particles by contributing additional surface charge and reduces the chances of coagulation. Without the surfactant, the collapsed chains coagulate and form lump (Camacho-Cruz et al., 2020).

Another mechanism which involves the entry of radicals into the monomer droplets and form latex particles is termed as droplet nucleation. In most of the conventional emulsion polymerization, due to relatively large monomer droplets, the surface area of monomer droplets is comparatively smaller than that of micelles, therefore droplet nucleation are not likely to occur in monomer droplets. Instead, an initiator molecule is more likely to interact with a free-floating monomer molecule before reaching a monomer droplet. In general, this relatively short stage creates stable seed particles which have an estimated diameter of 25 nm. These seed are then further expanded in stages that follow (Erlangung & Nazaran, 2008; Lovell & Schork, 2020).

### **2.3.2 Stage II (Particle growth)**

During stage II, the particles formed during nucleation become the loci for polymerization. Monomer molecules from the suspended monomer droplets in the system enter the micelles to create the seed particles. According to Harkins, monomer droplets exist and serve as reservoirs of monomer supply for growing latex particles by diffusion through the aqueous phase (Harkins, 1945). For monomers that have limited solubility in water, for examples n-butyl acrylate and methyl methacrylate, the monomer-swollen micelles, monomer droplets and the aqueous phase are in equilibrium to ensure that the free-floating monomers are in constant concentration.

When the concentration of free-floating monomer is low, monomer molecules migrate from the monomer droplets into the aqueous phase through diffusion. In the aqueous phase, monomers can also polymerize to form oligomers. These oligomers are insoluble in water at a critical chain length. Then, due to insufficient remaining surfactant to accommodate a new stable interface, these oligomers migrate towards the existing polymer particles' surface instead of forming new polymer particles. These polymer particles grow continuously by absorbing monomer molecules from monomer droplets in the aqueous medium via diffusion. (Asua, 2004; Bassett & Hamielec, 1981; Van Herk & Gilbert, 2013).

### **2.3.3 Stage III (Monomer finishing)**

Stage III happens when the monomer droplets are completely consumed and stop supplying monomer to the growing polymer particles. The concentration of monomers and rate of reaction also continues to decrease with time. During this stage, only polymer particles are present and further polymerization takes place. As the polymerization progresses, conversion increases, hence, the majority of polymer is formed. The final

product obtained at the end of Stage III is called latex (Chern, 2006).

On the other hand, auto-acceleration phenomenon or also known as Trommsdorff effect normally happened at this stage (Gilbert, 1995; Thickett & Gilbert, 2007). This phenomenon happens when the system turns viscous tremendously as the conversion increases. This is because in a viscous medium, the mobility of polymer chain radicals is limited, thus making them difficult to find each other to undergo termination. This can eventually cause generation of heat, resulting in a dramatic increase in temperature (Asua, 2004; Bassett & Hamielec, 1981; Van Herk & Gilbert, 2013).

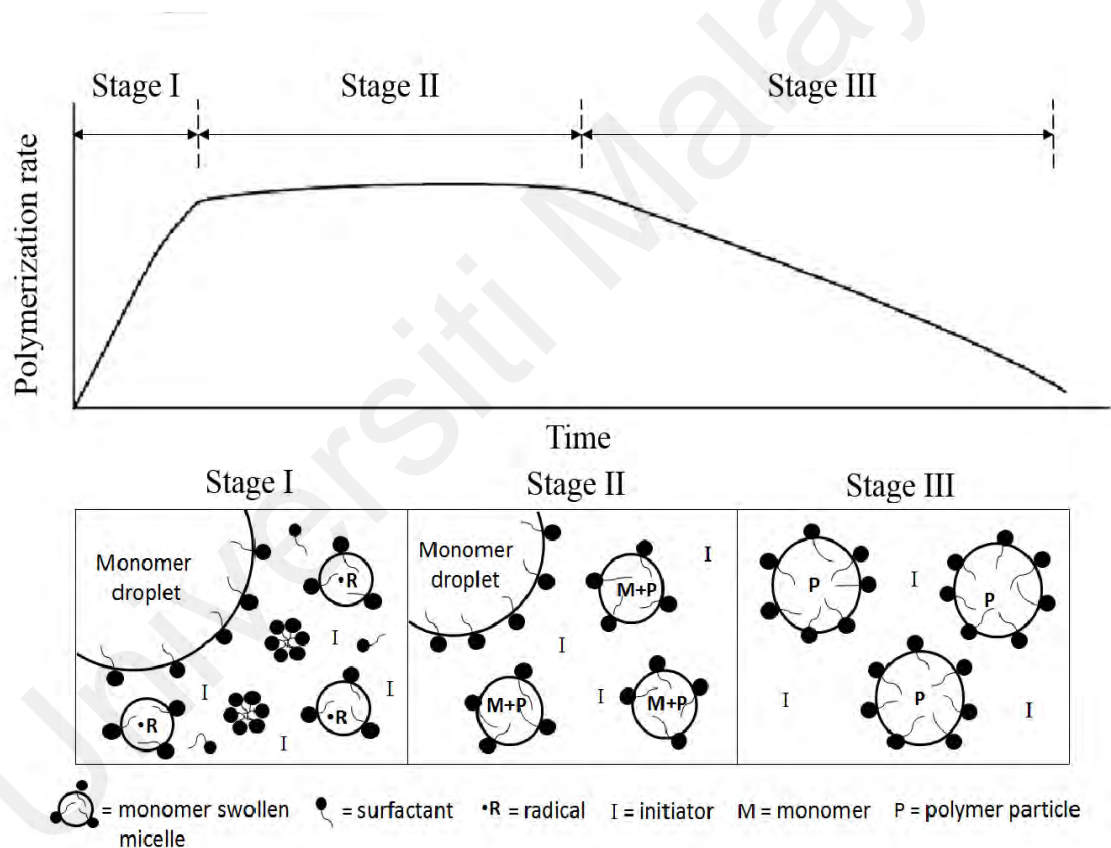


**Figure 2.2: Three main stages in emulsion polymerization**

## 2.4 In-situ seeded emulsion polymerization technique

In the past days' industrial emulsion polymerization, one of the primary challenges has been the irreproducibility in the number of nucleation of the latex particles and this is

known to influence the particle size and its distribution. One of the practices to avoid such fluctuations in batch-to-batch particle size is via an additional nucleation mechanism called 'seed latex' technology. It involves polymerizing monomers in a previously prepared latex with controlled amounts of emulsifier and initiator to create seed particles of larger size to avoid the generation of new particles (Lutz et al., 2012). Consequently, the particle size and particle size distribution of resulting polymer can be better-controlled. Seed latex can be created in situ or in a separate step and then fed into the reactor prior to polymerization. Since polymerization occurs only in the pre-formed seed particles which will grow to form the final particle, the size of the particles in the final product can be controlled to a certain extent.

For this polymerization technique, 5-10% of the total monomers are usually fed at the beginning of the reaction to create seed particles. Next, the remaining monomers can be introduced over time to grow the seed particles to a desired particle size via two methods: (1) direct addition or (2) pre-emulsion addition. Through direct addition, all surfactant is introduced at the initial seed stage, resulting in a higher number of seed particles. On the other hand, pre-emulsion addition will result in a lower number of seed particles due to lower surfactant concentration at the initial seed stage (Leiza & Meuldijk, 2013).

When the remaining monomers are added into the system, a secondary nucleation of particles might occur if the concentration of seed particles is too low and/or the concentration of surfactant is too high, resulting in a broad particle size distribution. On the other hand, if surfactant used is insufficient, the particle surface charge density will be too low to sufficiently stabilize the emulsion. This might eventually result in coagulation of particles, reducing the total number of particles at the end of polymerization (Bassett & Hamielec, 1981; Ito et al., 2002).

Normally, seeded emulsion polymerization is conducted as a semi-batch reaction

under monomer-starved conditions, whereby the monomer is being used up as fast as it is being fed. This is to make sure that after nucleation of seed particles, there are no leftover monomer droplets during Stage III where the entire polymerization occurs. In fact, during Stage I, a fixed number of particles are nucleated and when additional monomer is added, those particles propagate without nucleating additional particles. The number of seed particles undergo nucleation influences the particle size. For example, nucleation of less amount of seed particles yield larger particles; nucleation of a huge amount of seed particles yield smaller particles (Lovell & Schork, 2020; Nishida et al., 1981).

## **2.5 Glove coating application**

### **2.5.1 Origin of glove**

In the early 1900 s, rubber gloves have been introduced and their use had been adopted by surgeons in both Europe and the United States to protect the hands of operating theater personnel (Ownby, 2002). Over the last few decades, the wearing of gloves has become a common practice in the medical industry with the purpose of attaining good hygiene practices and to avoid cross-infections. Natural rubber (NR) latex, which is sourced from the *Hevea brasiliensis* tree, along with the synthetic raw materials, is frequently utilized in the production of medical gloves. In particular, NR benefits from excellent barrier properties against blood-borne pathogens, movement flexibility, resealing when perforated and a feasible cost performance ratio (Manhart et al., 2020; Yip & Cacioli, 2002). The usage of latex gloves in other aspects of daily life, such as food handling, also started to expand after 1987 (Ownby, 2002).

Rubber gloves are essential not only in providing a barrier of protection to the wearers' hands against infection diseases, but also to chemicals, abrasion or static electricity. The surface characteristics play a key role when it comes to donning properties, wearing

comfort, tactile sensation and dexterity of latex gloves (Mylon et al., 2014). One of the key criteria for a good glove is easy donning and should be comfortable while wearing. However, gloves fabricated from both natural rubber and synthetic nitrile rubber often suffered from donning difficulty due to their inherent tacky surface, causing high coefficient of friction between the skin and the surface of the glove. Thus, it has been the conventional practice to employ a layer of lubricant on the glove's inner surface to minimize donning difficulty.

## **2.6 Types of gloves coating**

### **2.6.1 Powdered gloves**

Earlier attempt to improve donning in gloves manufacturing is via the use of powder-based lubricants. Cornstarch powder or talc are commonly used to promote quick donning and to prevent the inner sides of gloves from sticking together (Preece et al., 2021). Typically, during production, the finished gloves that are still attached to the formers are dipped into a powder slurry tank, followed by drying and stripping from the formers. The powder slurry typically consisted of water, modified cornstarch, surfactants, magnesium oxide, biocides and other additives formulated by different manufacturers. However, one significant disadvantage of using powdered gloves is the high possibility of having the powder dislodged from the gloves resulting in contamination of samples, or even worse, in the case of surgical gloves, it may contaminate the wound and results in granuloma and other post-operative complications (Truscott, 2002).

On top of that, in the early 1990s, it was reported that the natural rubber latex (NRL) allergen can be absorbed by cornstarch powder and cause glove-associated allergic reactions in NRL allergic individuals (Truscott, 2002). The various adverse effects included:

- (i) Type I reactivity towards powder-based NRL protein allergens

- (ii) Type IV hypersensitivity to powder-absorbed chemical contact sensitizers
- (iii) Foreign body reactions
- (iv) Endotoxin-related consequences of powder-absorbed endotoxin

### **2.6.2 Chlorination**

Although the use of glove powder as a dusting lubricant to reduce the inherent tackiness of NR gloves still in practice, there is a growing demand for powder-free latex gloves, particularly chlorinated latex gloves. Compared to dusting powder which may easily fall off during usage, chlorination is a more permanent method of improving smoothness and reducing friction of the glove surface (Radabutra et al., 2009). Besides, this technique is widely used in the glove industry due to its low operational cost. It involves treating the rubber gloves with diluted chlorine solution during manufacturing to harden the surface of the rubber (Manhart et al., 2020; Preece et al., 2021). The chlorine solution could be prepared either by dissolving chlorine gas directly into water or by reacting a solution of hypochlorite with hydrochloric acid (Sen et al., 2001).

Nevertheless, there are several drawbacks of this technique. Romberg revealed that chlorination had a negative impact on the physical structure of the glove surface in addition to altering the chemical functioning of the surface. He also discovered cracks on the glove surface as a result of chlorination (Sen et al., 2001). Moreover, such cracks may result in a significant drop in the tensile strength of the NR latex glove. Worst case scenario happens when these cracks propagate further under extreme storage circumstances such as high temperature (e.g. in a tropical or arid climate), resulting to catastrophic deterioration. The usage of these deteriorating gloves might have serious implications for public health since pathogens or germs could be spread, especially during surgical procedures.

Apart from that, it is discovered that by chlorinating latex gloves compromises the surface morphology and mechanical properties such as tensile strength (Sen et al., 2001). As a consequence, it may reduce the grip, shelf life and in-use durability of the gloves. Over time, discoloration issue also might happen as the gloves deteriorate (Akabane, 2016). Another significant disadvantage is that chlorination beyond the optimum level might cause serious skin irritation among users, as well as generating unpleasant odor. Another significant limitation with the chlorination technique is the corrosion of the metallic part of the machineries involved in the process, which is not industrially-economical in the long term (Ong, 2001).

### **2.6.3 Polymeric coating**

The better option for powder-free gloves would be the application of a layer of polymer coating onto the glove surface (Davis, 1994). The polymer coating can be used to replace the powder as the donning lubricant. In industry, there are a wide range of polymers that have been used for the purpose, such as hydrophilic hydrogel; anionic polyurethane (Yeh, 2002); styrene-acrylic emulsions, and carboxylated styrene-butadiene emulsion. Although many different types of polymer coatings have been reported, not many of those reports involve detailed study on the effect of the monomers used on the properties of the polymer coating as well as the properties of coated rubber gloves (Modha et al., 2005). This is because other than improving donning lubricity, the coating material should also be able to serve other functions such as high resistance towards chemicals and solvents permeation, high tensile strength and strong adhesion, softness and flexibility, as well as excellent biocompatibility.

Several types of polymeric coatings have been developed for coating glove surfaces. For instance, Ansell et al discloses a blend of ionic polyurethane and a second polymer which can be another polyurethane or an acrylic polymer to be coated on hand



contacting surface of glove (Ansell et al., 1993). Another invention of Petrash et al. discloses polymer coating composition composed of a dispersant, microspheres, and a high  $T_g$  polymer for the inner coating of latex gloves (Petrash et al., 2004). In addition, other coatings such as emulsion copolymers have been disclosed by Janssen, whereby the polymeric material is made up of hydrophilic and hydrophobic monomers (Janssen, 2006). On top of that, Robert and Brackley found that hydrogel coating on gloves give a lower coefficient of friction than chlorination treatment, hence allowing easier donning (Roberts & Brackley, 1996). There is also a disclose that involves coating of polyisoprene layer on the elastomeric article which improved glove softness due to the chain flexibility of the polyisoprene segment (Chen et al., 2012). Recent advancement by Govindaraju introduced carboxylated styrene-butadiene latex having features such as higher hydrophobicity, rubber character and binding strength as coating material for NBR and NR gloves (Govindaraju et al., 2018).

The coating application often being carried out via “dipping” process. The term dipping is denoted as such due to the procedures involving formation of a thin coating by dipping an article into a liquid coating material (Ong, 2001). This technique is particularly useful to coat irregularly shaped items, such as gloves, catheters, or feeder teats for babies. The dipping process may also be used to produce flexible, thin-walled articles from natural or synthetic polymers (Sornsanee et al., 2018). During the dipping process, a suitable shape, industrially known as a “mold”, “form”, or “former”, is dipped into a latex for an appropriate dwelling period. Next, the coated former is then heated to dry and cure the polymer. In the final step, the article is removed from the former, retaining its shape (Akabane, 2016). As a result, the dipping process enables the formation of seamless thin-walled products with specified or sometimes, complex geometries. General process flow involved in manufacturing of polymer-coated rubber gloves as shown in the Figure 2.3.

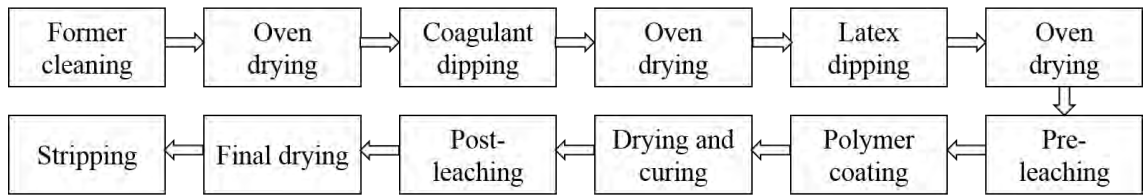


**Figure 2.3: General process manufacture flow of polymer-coated rubber gloves in industry**

## 2.7 Properties of polymer coating on rubber films

In surface coating application for gloves, polymeric resins offer various advantages owing to their structural characteristics. Surface coating is commonly used to produce film of desired properties and functions such as surface smoothness, film flexibility and surface adhesion.

### 2.7.1 Surface smoothness

Surface smoothness can be determined by measuring the coefficient of friction (CoF) of the polymer coated rubber articles. CoF is the key parameter used to measure the amount of friction between two surfaces (Zhang, 2016). The CoF value is a dimensionless number in which the value is given by taking the ratio between frictional force and normal force:

$$\text{CoF} = \text{frictional force (F)} / \text{normal force (N)} \quad (2.1)$$

Lower CoF value means less force was needed to slide an object on the surface of the test sample, and the opposite applies. Typically, materials with CoF lower than 0.1 are considered as lubricous materials (Zhang, 2016). In the case of polymer coating for gloves, the CoF value is typically below 0.2 (Govindaraju et al., 2018). CoF relies on the materials' nature and roughness of the surface. Typically, the most widely used standard test method to measure CoF is ASTM D189-14. In this method, a fixed weight is placed on top of the specimen film on a stainless steel. Then, the weight is allowed to slide across

the specimen film and the frictional force needed to pull the weight is measured during the sliding. In this test, the normal force is equal to the weight's gravitational force.

### **2.7.2 Film flexibility and surface adhesion**

Next, film flexibility and good surface adhesion also need to be considered when designing the formulation of polymer coating for gloves. The types and ratio of monomers used play a decisive role for the films' mechanical property, level of hardness and flexibility (Zhang et al., 2017). Monomers with higher  $T_g$  such as styrene and methyl methacrylate are hard monomers that derive hardness and abrasion resistance, as well as provide cohesion to the latex film. Meanwhile, soft monomers such as n-butyl acrylate and isooctyl acrylate have lower  $T_g$  that give latex film flexibility and surface adhesion (Zhong et al., 2013). For instance, Drake et al. found out that the tensile strength and elongation decrease with increase in butyl acrylate content (Drake et al., 2019). On top of that, the hardness of the resin can be enhanced by increasing the content of styrene as reported by Sherif et al for paper coating (El-Sherif et al., 2019). In glove's polymer coating application, film with good flexibility and surface adhesion is preferable.

Flaking is one of the most common issues faced by the glove manufacturer when polymer is coated on the inner surface of gloves. Flaking, also known as cracking or delamination means a fissure in the surface of the coating that may or may not extend through the entire thickness of the coating to the underlying elastomeric substrate (Chen et al., 2015). Flaking can occur either when the rubber article is stretched at normal force or overly-stretched. Significant difference in elasticity between the polymer coating and rubber article or poor bonding might cause flaking of the polymer coating during processing and donning. Polymer coating which has poor adhesion to the rubber article will delaminate easily from the surface of the rubber article, which will cause the tackiness of the donning surface. The flaking of the coating on the rubber article can be

inspected visually by observing for the presence of powdery substance on the surface of the rubber article.

## **2.8 Film formation mechanism**

The process of film formation from latex or aqueous based polymeric dispersions underlies much of the water-borne coatings technology. At sufficiently high temperature, a transparent film coating is formed after applying latex dispersions on the substrate. At lower temperature, stiff, cracked or powdery films are formed. Thus, the minimum film forming temperature (MFFT) has been widely recognized as the crude measure of the deformability of the particles during the drying period, and is mostly related to the glass transition temperature of the latex polymer (Winnik, 1997). At temperature below MFFT, the polymeric dispersion forms an opaque, discontinuous material upon solvent evaporation, meanwhile, above the MFFT, a clear continuous film is formed. However, polymer solutions do not exhibit a MFFT and will form a film at room temperature (Felton, 2013).

The film formation mechanism involves three main stages as shown in Figure 2.4: (i) water evaporation, (ii) particle deformation and finally, (iii) coalescence and polymer chain interpenetration (Ramos-Fernández et al., 2012). Initially, after applying the dispersion to the substrate, water will evaporate off the surface and the polymer particles become more concentrated and pack together in a close arrangement. At this early stage, the rate of evaporation of water is constant (Steward et al., 2000). Next, when the forces accompanying drying exceed the modulus of the polymer particles, the particles deform to fill in the void spaces left by the evaporating water. A void-free film is formed, yet is still mechanically weak. In the final stage of film formation, coalescence happens where the polymer particles flow together and the polymer chains interpenetrate to provide the entanglements that contribute strength to the film (Winnik, 1997).

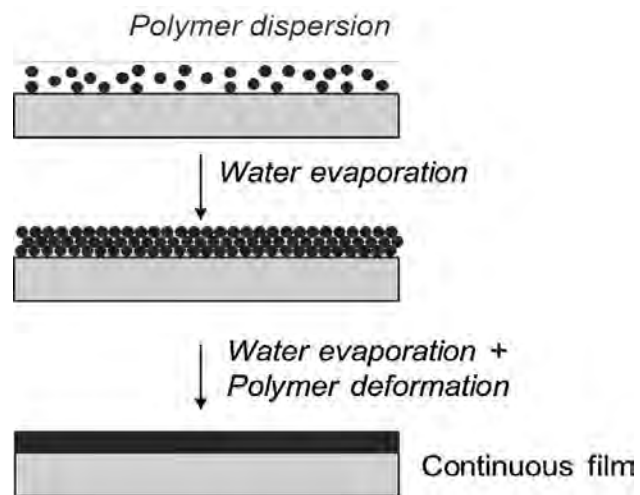


**Figure 2.4: Three main stages involved in film formation mechanism**

## CHAPTER 3 : EXPERIMENTAL

### 3.1 Materials

Styrene (St), butyl acrylate (BA), and isoprene (Iso) monomers purchased from Merck, Germany were washed with 2 w/v % sodium hydroxide (NaOH) solution first, followed by distilled water to remove the inhibitor. Acrylic acid (AA), potassium persulfate (KPS) and deuterated chloroform ( $\text{CDCl}_3$ ) were purchased from Sigma Aldrich, USA. Sodium dithionite ( $\text{Na}_2\text{S}_2\text{O}_4$ ) and concentrated aqueous ammonia (28-30%) were purchased from Merck, Germany. Sodium dodecyl benzene sulfonate (SDBS) solution of 30 % solid content, and calcium nitrate aqueous solution were obtained from Top Glove Sdn. Bhd, Malaysia. Industrial grade methanol was purchased from Kofa Chemical Works (M) Sdn. Bhd, Malaysia. Unless otherwise specified, all chemicals used were of analytical grade and used as received. Prior to the synthesis, distilled water used was purged with nitrogen gas.

### 3.2 Apparatus

Figure 3.1 shows the apparatus set-up for the emulsion copolymerization of St-BA-Iso emulsion copolymer in a 2 L five-necked round-bottomed flask secured in a water bath. The flask was equipped with a reflux condenser to minimize loss of monomers via evaporation, a mechanical stirrer for agitation, a digital thermometer to observe the reaction temperature from time to time, and two dropping funnels to feed the monomers and initiator solution simultaneously. A thermoregulator was used to control the temperature of water bath and the temperature was set at  $70 \pm 2^\circ\text{C}$ .

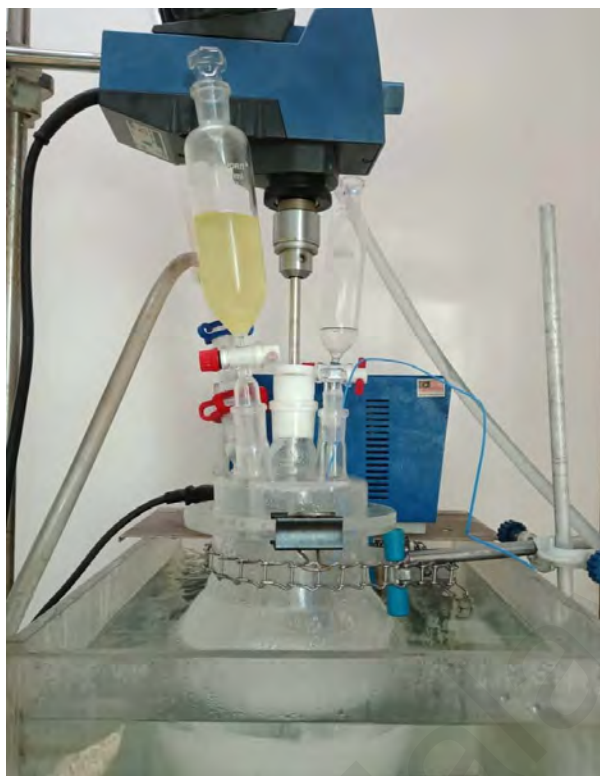


**Figure 3.1: Experimental set-up for emulsion polymerization**

### 3.3 Synthesis of St-BA-Iso emulsion

A series of six emulsions of varied monomers composition were prepared with a targeted solid content of  $40 \pm 3$  %. Table 3.1 summarizes the basic properties of the three main monomers used in this study: styrene (St), butyl acrylate (BA) and isoprene (Iso). The composition of monomers used was tabulated in Table 3.2, and the complete recipe for the synthesis is shown in Table 3.3.

**Table 3.1: Literature value of monomers' properties**

Monomer	Molecular weight (g/mol)	T <sub>g</sub> of homopolymer (°C)	Density (g/mL)
St	104.15	100	0.909
BA	128.17	-54	0.894
Iso	68.12	-61	0.680

(Germack & Wooley, 2007; Lutz et al., 2012)

**Table 3.2: Monomer compositions of a series of St-BA-Iso emulsion copolymer**

	St-BA-Iso emulsion copolymer					
	St-60	St-40	BA-60	BA-40	Iso-60	Iso-40
<b><u>Monomer composition</u></b>						
<b><u>(wt. %)</u></b>						
Styrene	58.5	38.5	20.0	30.0	20.0	30.0
Butyl acrylate	20.0	30.0	58.5	38.5	20.0	30.0
Isoprene	20.0	30.0	20.0	30.0	58.5	38.5
Acrylic acid	1.5	1.5	1.5	1.5	1.5	1.5

**Table 3.3: Detailed formulation on the synthesis of St-BA-Iso emulsion copolymers**

Samples	Mass of ingredients introduced (g)					
	St-60	St-40	BA-60	BA-40	Iso-60	Iso-40
<b><u>Monomers</u></b>						
Styrene	292.5	192.5	100.0	150.0	100.0	150.0
Butyl acrylate	100.0	150.0	292.5	192.5	100.0	150.0
Isoprene	100.0	150.0	100.0	150.0	292.5	192.5
Acrylic acid	7.5	7.5	7.5	7.5	7.5	7.5
<b><u>Anionic surfactant</u></b>						
SDBS (30% TSC)			57.3			
<b><u>Initiator</u></b>						
KPS (0.04 M)			188.7			
<b><u>Activator</u></b>						
Na <sub>2</sub> S <sub>2</sub> O <sub>4</sub> (0.004 M)			100.5			
<b><u>pH regulator</u></b>						
NH <sub>3</sub> (aq)			5.5 – 6.5			
<b><u>Reaction medium</u></b>						
Distilled water	315	296	311	295	244	280



Firstly, in the round-bottom flask, a solution comprising the calculated amount of SDBS surfactant and water was added. The mixture was heated up to  $70 \pm 2$  °C with stirring at constant agitation at 100 rpm. To create seed emulsion, 20 % of the total amount of monomers was charged directly into the flask, followed by a 20 min stirring. Next, 20 % of the initiator-activator solution which consisted of the total amount of KPS and  $\text{Na}_2\text{S}_2\text{O}_4$  was charged directly into the flask. The reaction mixture was allowed to stabilize and form seed emulsion for another 20 min. The rest of the monomers and initiator-activator solution were continuously fed dropwise and concurrently into the flask over a period of 5 h. At this stage, the temperature of the reaction was maintained, while the agitation speed was slightly increased to mild stirring at around 200 rpm to homogenize the emulsion and avoid coagulation. Once the feeding completed, the reaction mixture was allowed to polymerize for another 4 h at constant temperature and stirring speed. The emulsion was left to cool to room temperature, neutralized with ammonia solution, and finally filtered through filter cloth and stored in a storage bottle. The proposed structure of St-BA-Iso emulsion copolymer is as shown in Figure 3.2.

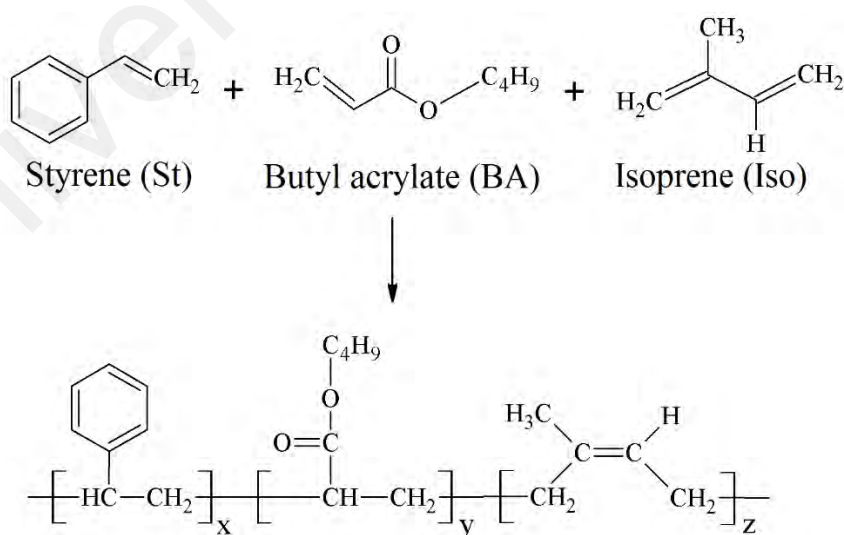


**Figure 3.2: Proposed structure of St-BA-Iso copolymer**

### 3.4 Characterization of St-BA-Iso emulsion

#### 3.4.1 Extent of conversion and total solid content (TSC)

Aqueous calcium nitrate solution was used as the coagulant to precipitate out a small amount of the synthesized emulsion,  $M_0$ . With a Buchner funnel, the precipitate was filtered and washed using distilled water, followed by methanol in excess. The precipitate was then dried in the vacuum oven at 80 °C for 2 h and the final dried mass was weighed,  $M_1$ . Three sets of data were collected for each sample and the extent of conversion and TSC % were determined using the following equations:

$$\text{Extent of conversion (\%)} = \frac{M_1}{M_0 \cdot \alpha} \times 100 \% \quad (3.1)$$

$$\text{TSC (\%)} = \frac{M_1}{M_0} \times 100 \% \quad (3.2)$$

where  $\alpha$  = mass ratio of monomer to emulsion.

#### 3.4.2 pH value

A standard digital pH electrode with Ag/AgCl reference electrode and a glass electrode was used to determine the pH of the emulsions. The equipment was calibrated with buffer solutions prior to measurement. Three sets of measurement were recorded, and the average values were reported.

#### 3.4.3 Surface tension

Surface tension of the emulsions were determined using Wilhelmy plate method. The Wilhelmy plate is a thin, rectangular plate made of iridium-platinum with 23.87 mm width and 0.17 mm thickness. During the test, the Wilhelmy plate were dipped into the emulsion and then pulled back to the interface, forming a liquid lamella. The weight of the liquid lamella formed and the interfacial tension were calculated automatically using a surface tension analyser (SEO DST60M, Korea).

### 3.4.4 Particle size

The average particle size of the copolymer emulsions was determined using laser scattering particle size distribution analyser (Horiba LA960A, USA) as shown in Figure 3.3. The central concept in laser diffraction method involves light scattering by a particle, and this process is dependent on the particle's size. A collection of particles produces a scattered light pattern defined by intensity and angle that can be converted into particle size distribution curve. To conduct the analysis, the emulsion can be used directly by dispersing each emulsion samples into the sampling bath containing deionized water. The sample bath was allowed to stabilize before subjected to measurement.



**Figure 3.3: Particle size analyser Horiba LA960A**

### 3.4.5 Zeta potential

The zeta potential of the emulsions was measured using zeta potential analyser (Malvern Nano ZS, Germany) as shown in Figure 3.4 at 25 °C. The emulsions were firstly diluted in ultrapure water at 1:1000 (v/v) proportions, followed by transferring them into an electrophoretic mobility measurement sample cell (capillary cell). The type of capillary cell used for the test was DTS1070. In the capillary cell, there are electrodes at both ends of a closed tube. This type of cell is particularly excellent for aqueous applications, whereby the measurement position is distant from the electrodes, avoiding

any bubbles and interference from electrolysis when measuring samples of high conductivity. For each emulsion, three measurements were taken and the average zeta potential value were automatically calculated from the software.

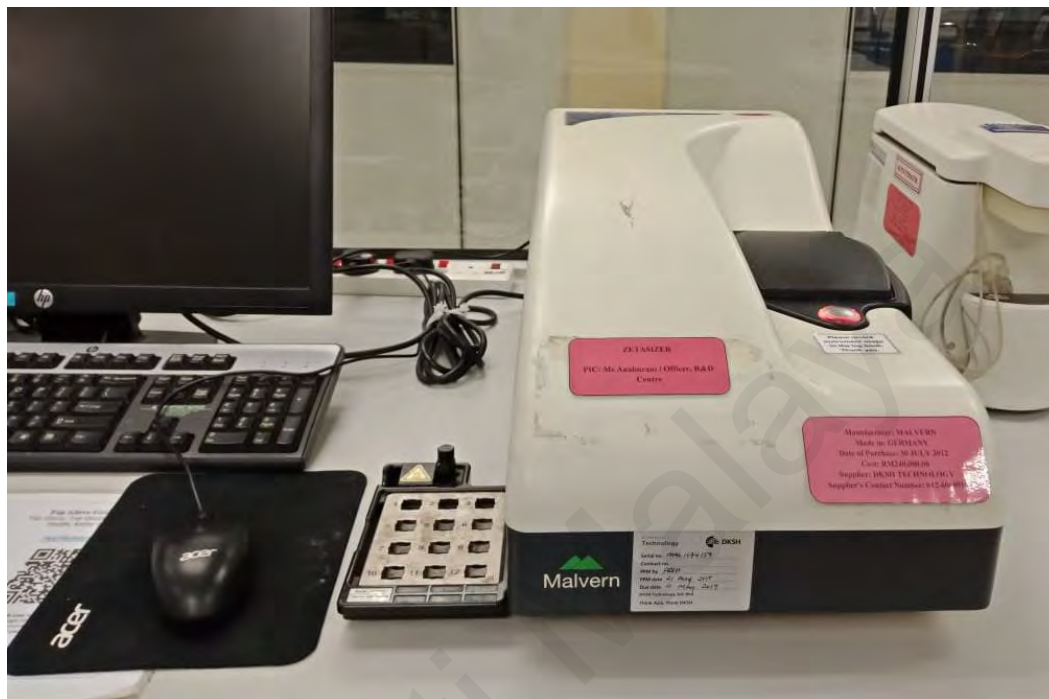


**Figure 3.4: Zetasizer Malvern Nano ZS**

### **3.5 Characterization of St-BA-Iso copolymer**

#### **3.5.1 Attenuated total reflectance – Fourier transform infrared (ATR-FTIR)**

FTIR spectroscopy is an analytical technique used to perform characterization and identification of unknown materials such as liquids, solids, powders, and films. A change in the material composition results in a change in the characteristic pattern of absorption bands. In this work, spectroscopic characterization of the dry copolymer film samples was carried out using ATR-FTIR spectrometer (Perkin Elmer FTIR-Spectrum 400, USA) as shown in Figure 3.5. In practice, the films were directly placed on the diamond-shaped sample holder before running the measurement. The analysis was done with 8 scans, ranging from 400 to 4000  $\text{cm}^{-1}$  at resolution of 4  $\text{cm}^{-1}$ .



**Figure 3.5: Perkin Elmer ATR-FTIR spectrum 400 spectrometer**

### **3.5.2 Proton Nuclear Magnetic Resonance ( $^1\text{H}$ -NMR)**

NMR spectroscopy is among the most powerful and extensively used analytical techniques in chemical research for investigating structures and dynamics of molecules. It can also be used in quality control to determine the purity and content of a sample. In this study,  $^1\text{H}$ -NMR of 400 MHz resonance (JEOL ECX 400, USA) as shown in Figure 3.6 was used to elucidate the chemical structure of the synthesized copolymer. Before running the analysis, all copolymer samples were soaked in deuterated chloroform ( $\text{CDCl}_3$ ) in 2:1 mass ratio of copolymer: solvent and left overnight. The sample solutions were then filtered before introduced into 7-inches NMR tube. The height of the sample in each of the NMR tube was at least 4.0 to 4.5 cm, and each analysis involves 16 scans.



**Figure 3.6: JEOL 400 MHz resonance spectrometer**

### **3.5.3 Gel Permeation Chromatography (GPC)**

GPC is a type of size exclusion chromatography and it is commonly used to determine the molecular weight distribution of a polymer. It involves passage of a dilute polymer solution over a column of porous beads, whereby polymers of higher molecular weight are excluded from the beads and elute first, while lower molecular weight polymers are able to pass through the porous beads, slowing the elution process. The molecular weight of the copolymer samples was measured using gel permeation chromatography, GPC (Waters e2695, USA) as shown in Figure 3.7. 10 mg of the copolymer samples were weighed and dissolved in 10 mL of THF, and the samples were allowed to swell in the THF solvent overnight before it is filtered through a PTFE membrane with pore size of 0.45  $\mu\text{m}$ .



**Figure 3.7: GPC Waters e2695**

#### **3.5.4 Thermogravimetric Analysis (TGA)**

TGA is a basic thermal analysis technique to evaluate the thermal stability and composition of a material. It operates by measuring the amount and rate of weight change with respect to temperature change in a controlled atmosphere. In this study, this characterization was intended to analyse the thermal degradation of St-BA-Iso copolymers, as well as to evaluate their thermal stability. TGA was carried out using thermogravimetric analyser (Perkin Elmer TGA 4000, USA) as shown in Figure 3.8. The TGA consists of a sample holding pan that is connected to a precision balance and the entire set up is within a furnace. For the analysis, approximately 10 mg of each samples was placed on a ceramic sample pan and heated in the temperature range of room temperature ( $\sim 30^\circ\text{C}$ ) to  $900^\circ\text{C}$  at a heating rate of  $20^\circ\text{C}/\text{min}$ , under nitrogen atmosphere. TGA thermograms of each sample was plotted as weight percentage versus temperature.



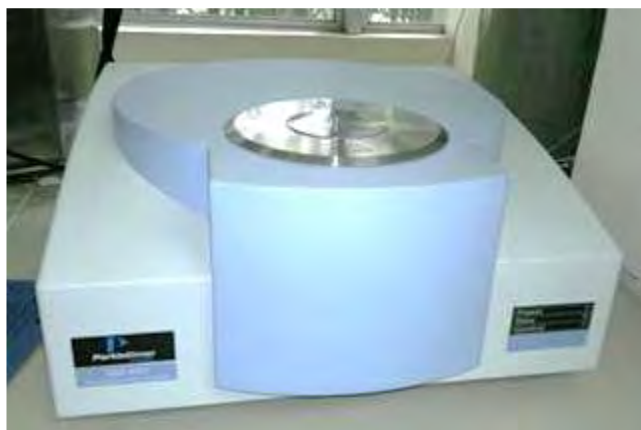


**Figure 3.8: Perkin Elmer TGA-4000**

### **3.5.5 Differential Scanning Calorimetry (DSC)**

DSC is a powerful thermoanalytical tool which can be used to identify various physical properties and thermal transitions of polymeric substances. DSC analysis was performed using differential scanning calorimeter (TA Instruments DSC Q20, USA) as shown in Figure 3.9 to measure the glass transition temperature ( $T_g$ ) of each St-BA-Iso copolymer film samples. To perform the analysis, approximately 10 mg of each sample was weighed and placed into an aluminium sample pan. The pan was then placed into the sample chamber inside the furnace, along with an empty aluminium pan which acts as reference. The sample chamber is equipped with detector to monitor the difference in the heat flow between the sample pan and reference pan, measuring the heat change of the samples as a function of time. DSC measurement was conducted at temperature ranging from  $-70\text{ }^{\circ}\text{C}$  to  $100\text{ }^{\circ}\text{C}$  with heating rate of  $20\text{ }^{\circ}\text{C}/\text{min}$ , under nitrogen atmosphere.





**Figure 3.9: TA Instruments DSC Q20**

### 3.5.6 Tensile test

A tensile test is a mechanical test involving the application of tension to a specimen until it fractures. It is typically used for determining a material's tensile strength, elongation to break and ductility. Tensile testing machines are also known as universal testing machine. In this study, to evaluate the mechanical properties of the copolymer, tensile test was conducted using universal testing machine (Sirius HEXA-6, China) as shown in Figure 3.10. The test was conducted according to a standard method EN455-2 (Kramer & Assadian, 2016). Prior to the test, the copolymer emulsions were dried at room temperature to obtain thin copolymer films. The films were then cut into dumbbell-shaped specimens with a gauge length of 20 mm and 3 mm width using a dumbbell cutter. To run the test, each end of the specimen was gripped in the tensile testing machine, where tension with a crosshead speed of  $500 \text{ mm min}^{-1}$  was applied until the specimen breaks. The testing was conducted in a controlled environment with relative humidity of  $50 \pm 10 \%$  and temperature of  $23 \pm 2 \text{ }^{\circ}\text{C}$ . All the samples were duplicated and the average value was reported.



**Figure 3.10: Universal testing machine Sirius Hexa-6**

### **3.6 Polymer coating on rubber film**

#### **3.6.1 Compounding of St-BA-Iso polymer coating solution**

The obtained St-BA-Iso emulsions were compounded into a 20 % TSC polymer coating solution and further diluted to 2 % TSC before proceeding to rubber film coating. A calculated amount of emulsion, pre-mix additive, pH adjustor and water were weighed and added into a beaker to prepare a 20 % TSC of polymer compounding mixture. The mixture was allowed to stir at 500 rpm until all the additives were completely dissolved and achieved homogeneity. Next, a calculated amount of hydroxyethyl cellulose which acts as thickening agent were gradually added into the polymer compounding mixture while stirring. As the mixture gets thicker and viscous, the stirring speed was gradually increased, and the mixture was left to stir until it became homogenous. Lastly, the mixture was further diluted to 2 % TSC, filtered with filter cloth, and ready for rubber film coating (refer Figure 3.11). The compounding formulation to prepare a 20 % TSC polymer

coating solution is as detailed in Table 3.4:

**Table 3.4: Compounding formulation**

Ingredients	Function	TSC %
Emulsion/resin	Binder	14.02
Pre-mix additive	Properties modifier	4.84
NH <sub>3</sub> aq.	pH adjustor	0.40
Hydroxyethyl cellulose	Thickening agent	1.20
Water	Dispersion medium	-
Total		20.00



**Figure 3.11: 2% TSC polymer coating solution**

### 3.6.2 Preparation of rubber film coated with St-BA-Iso copolymer

The process flow of lab-scale rubber film preparation is mostly similar to that of industrial scale as mentioned earlier in the literature review (refer Figure 2.3), except for the usage of ceramic plates as the mold in lab-scale practice instead of the actual hand-shaped formers. Firstly, ceramic plates were thoroughly cleaned prior to the preparation of rubber films. The cleaned ceramic plates were then pre-heated to dry, followed by dipping in calcium nitrate coagulant solution at 55 – 60 °C for 10 s. The coagulant-coated plates were dried in oven at 120 °C for 15 min.

Next, the coagulant-deposited ceramic plates were gently dipped into compounded NR latex over a dwelling period of 10 s. The latex-coated plates were then placed in the oven for 1 min at 120 °C which gelled the latex, followed by dipping the film in hot water (70 °C) for 20 s to leach out water soluble materials such as calcium nitrate from the film. Next, the leached films were then dipped in the compounded St-BA-Iso polymer coating solution that has been diluted to 2 % TSC for 10 s. The excess polymer coating solution was made sure to dripped out from the latex surface to ensure a uniform polymer coating layer was formed.

The polymer-coated plates were then placed in the oven at 120 °C for 15 min to allow curing and vulcanization of rubber to takes place. The cured rubber films were then further leached in hot water to extract out the remaining water-soluble components, followed by final round of oven drying at 120 °C for 3 min. After cooling down to room temperature, the rubber films were manually stripped from the plates, whereby they were turned inside out with the St-BA-Iso coated surface on the donning side. In industrial scale, a hand-shaped former is typically used as the mold. The idea of dipping process is illustrated as shown in Figure 3.12, while Figure 3.13 shows a part of the processes involved for lab-scale dipping of rubber films.

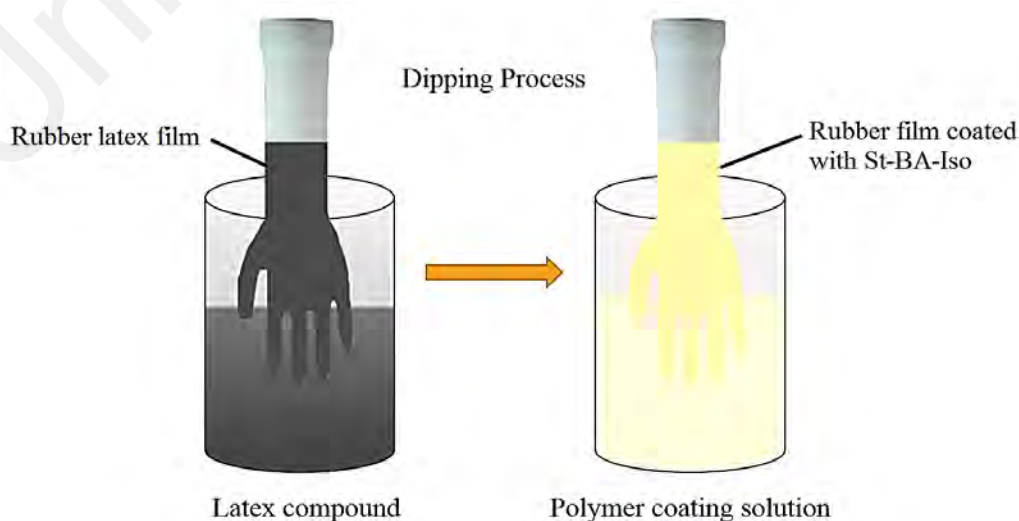


**Figure 3.12: Illustration of dipping process involved**



**Figure 3.13: Lab-scale dipping setup**

### **3.7 Properties of coated rubber film**

#### **3.7.1 Coefficient of friction (CoF)**

Coefficient of friction of the polymer coated rubber films were measured with CoF tester (Leading Instruments COF-02) as shown in Figure 3.14 using a sled of 200 g with testing speed of 150 mm/min. The method employed was adopted from ASTM D1894-14. The donning side of the rubber film was cut into specimen piece and was attached to the sled. Another specimen piece was placed onto the testing surface, and the sled was then allowed to slide against it. Three consecutive readings were recorded, and the average result was reported.



**Figure 3.14: Leading Instruments COF-02**

### 3.7.2 Physical tests and visual inspections

Physical inspection was also carried out on the polymer coated rubber films to evaluate its tackiness and to complement the result from CoF test. To evaluate the film tackiness, the donning surface of the films was rubbed together with pressure using thumb and index finger. The donning surface is considered tacky if there is resistance felt during the rub.

Blocking test was carried out by conditioning the coated rubber glove in oven at 70 °C for 24 h (Ab Rahman et al., 2020; Rahman et al., 2020). The condition set is to serve as a simulation to real-time aging at ambient temperature. It is known as the short-term accelerated aging method which offers an advantage to estimate a more liable and conservative shelf life that supports a practical shelf life. Via blocking test, the performance of the coating on the rubber was evaluated based on the stickiness of the donning surface at the end of the heat treatment. A good coating is expected to remain tack-free throughout the test.

The adhesion and rigidity of the polymer coating on the rubber glove was qualitatively evaluated by stretching the coated rubber film, and subsequently observe for any defects such as formation of white patch, cracking, or delamination. Water turbidity test which was adopted from (Myre & Shaw, 2006) was also carried out to evaluate the film adhesion of the coating on the rubber film. The test evaluates the level of difficulty of the polymer coating to be rubbed off from the rubber film. First, the rubber film was overly stretched, followed by rubbing it with 10 mL of water for 20 s. The water was then poured into a conical flask which was placed on top of a “X” mark (Figure 3.15) to check the level of water turbidity. Highly turbid solution indicates that the polymer coating delaminates easily from the rubber film, mainly due to poor coating adhesion.





**Figure 3.15: 'X' mark for water turbidity test**

### 3.7.3 Scanning Electron Microscope (SEM)

SEM is an instrument that provides surface structure and morphology of a samples by scanning the sample surface with a focused beam of electrons. The morphology of the coated rubber films was examined by scanning electron microscopy, SEM (JEOL JSM-6010LV, Japan) under low vacuum mode with electron acceleration voltage of 15 kV and magnification of 1 mm. For the analysis, the sample position was ensured straight and electron column was closed after inserting the stub into the sample chamber inside the electron column as shown in Figure 3.16 (a). Prior to the analysis, the rubber films were coated with gold powder using a gold coater (Smart Coater JEOL, Japan) as shown in Figure 3.16 (b) to acquire images of better resolution. Images of the rubber films before and after stretched were captured to observe the flakiness, delamination and/or formation of cracks.

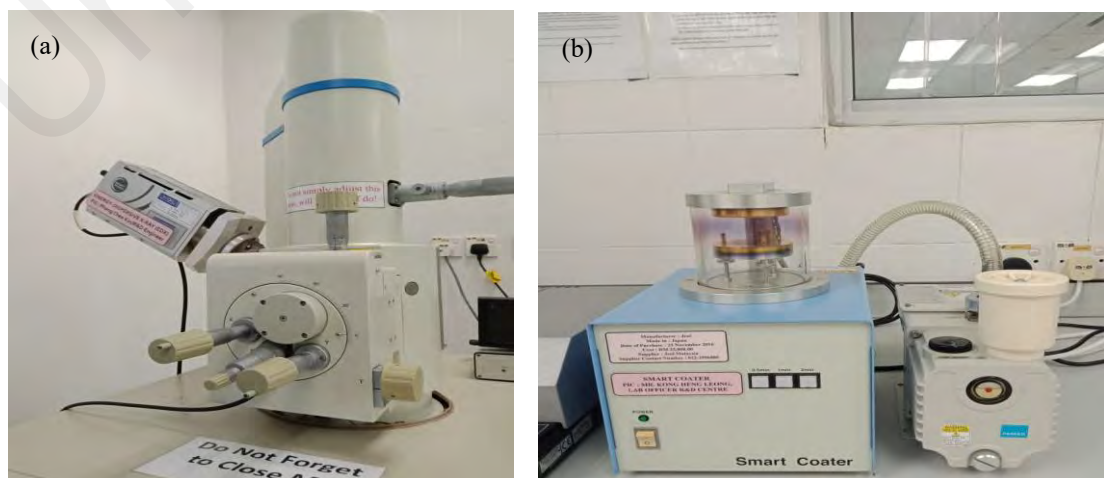


**Figure 3.16: (a) JEOL JSM-6010LV SEM sample chamber, (b) JEOL gold coater**

## CHAPTER 4 : RESULTS AND DISCUSSION

### 4.1 Characterization of St-BA-Iso emulsion

#### 4.1.1 Extent of conversion and TSC %

Extent of conversion and total solid content (TSC %) were calculated according to equation 3.1 in Chapter 3.0. All experimental values are in close agreement with targeted values. Table 4.1 presents the extent of conversion and TSC % of the synthesized emulsions. All the synthesized latexes appeared as milky white emulsion, and mostly exhibited conversion well above 90 %, and TSC in the range of  $41 \pm 2$  wt. %, except for Iso-60. A slightly lower % conversion and TSC % observed in Iso-60 is due to the loss of some isoprene monomer during the synthesis as it has considerably lower boiling temperature ( $34.07\text{ }^{\circ}\text{C}$ ) than the temperature of the polymerization (Songsiri et al., 2019). However, in most latex applications, it is conventional to have an emulsion with solid content ranges from 30 to 50 % as this could balance up the production efficiency as well as to maintain suitable viscosity of the product for ease of processing (Zubitur & Asua, 2001). Producing emulsion with very low TSC is not industrially friendly because the amount of polymers content obtained in the emulsion is low and does not justify the long duration of time needed for the synthesis. On the other hand, emulsion of very high TSC tend to be very viscous, which in turn impacts heat removal, mass transfer, and there is also higher possibility that the coagulum form during the production (Mariz et al., 2011).

At the end of each synthesis, the pH of St-BA-Iso emulsion tend to be relatively low, in the range of pH 4 to 5, and it was subsequently adjusted with ammonia solution to pH close to 7.0 for stability purpose (Jauregui, 2016). The surfactant used in this study is anionic in nature, and it is well understood that excessive concentration of  $\text{H}^{+}$  ions in acidic medium would eventually neutralizes the charge of the surfactant and increase odds of direct collision among the latex particles, destabilizing the emulsion and results with conglomeration (Li et al., 2016).



**Table 4.1: Conversion and TSC % of St-BA-Iso emulsions**

Samples	Conversion (%)	TSC (wt. %)
St-60	92.3	39.7
St-40	95.2	41.7
BA-60	100.0	43.4
BA-40	96.9	42.5
Iso-60	80.5	36.9
Iso-40	91.2	40.5

#### 4.1.2 Physical properties

In coating application, the value of surface tension gives an indication of how well the coating can be distributed on a substrate. Resin with lower surface tension typically leads to better coating uniformity (Yekeen et al., 2020). As shown in Table 4.2, Iso-60 emulsion has the lowest surface tension of  $37 \text{ N m}^{-1}$ , while the remaining of the emulsions recorded similar surface tension value,  $51 \pm 3 \text{ N m}^{-1}$ . Based on the appearance of the films shown in the later part of this work (Figure 4.22 (a)), all six emulsions produced reasonably uniform coatings.

Particle size has direct influence on the physical stability of an emulsion, in which a system with smaller dispersed particles tend to be more stable (de FA Mariz et al., 2010). With smaller size, more particles can participate in film formation around the droplets in the dispersed phase, resulting in a more stable emulsion (Iyer et al., 2015; Tadros, 2013). Particle size distribution curves for all samples are shown in Figure 4.1. The curve produced a relatively narrow unimodal distribution of the particle size in all six emulsions. This could be attributed to the advantage of seeded emulsion polymerization technique that was used in this work. By applying seeded emulsion polymerization technique, the monomers were fed into the system in starved condition, where the monomers were introduced gradually into the reaction vessel at a rate that allowed majority of the monomers to be consumed by the reaction before more were added. In

this way, the first few percent of monomers are able to achieve controlled particle growth without any secondary nucleation, and subsequently preventing possible coagulation of the particles (Lovell & Schork, 2020; Mariz et al., 2011).

The size of the particles in the emulsions are small and comparable to each other, with all of them having mean size in the range of  $82 \pm 4$  nm. Detailed analysis on the particle size, shown in Figure 4.2, reveals that St-60 and St-40 emulsions have smaller particle size than the rest, and they are expected to be more stable. Although minimal, difference in the mean size of the particles between the emulsions is notable, with Iso-40 recording the highest mean size of 86.0 nm while St-60 has the smallest mean size of 78.5 nm. The difference in the size may be attributed to the difference in the initiation reactivity of the monomers. Styrene which comprised of aromatic ring attached to a vinyl unsaturation can form a relatively stable radical intermediate, and this explains the relatively high tendency of the monomer to form radical (Jianying et al., 2006). Formulation with higher loading of styrene such as St-40 and St-60 would therefore have higher concentration of radicals formed at a time, resulting with more active sites for polymer chains to grow. Consequently, there are more particles formed in the system and they tend to be relatively smaller in size.

**Table 4.2: Physical properties of St-BA-Iso emulsions**

<b>Samples</b>	<b>Final pH</b>	<b>Surface tension (N/m)</b>	<b>Mean size (nm)</b>	<b>Median size (nm)</b>	<b>Zeta potential (mV)</b>	<b>M<sub>w</sub> (Daltons)</b>
St-60	6.7	53.7	78.5	74.3	-46.5	77642
St-40	6.5	51.0	80.0	75.2	-41.5	67715
BA-60	6.9	48.0	85.5	81.5	-48.3	44626
BA-40	6.8	49.7	85.1	81.3	-49.0	84623
Iso-60	7.0	37.0	84.7	80.7	-35.2	57463
Iso-40	6.9	48.6	86.0	81.8	-55.1	64330

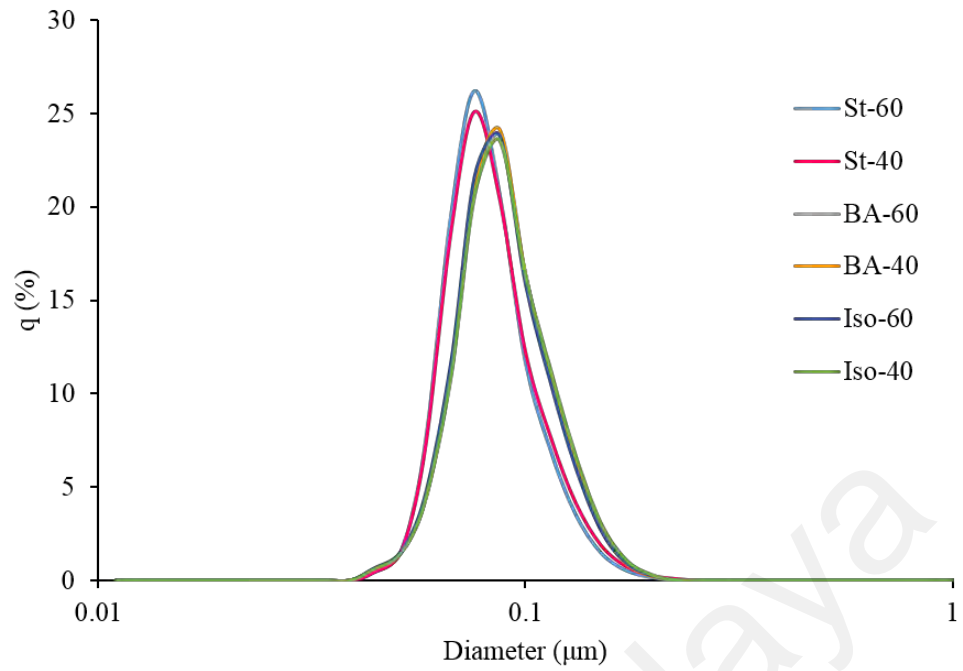


**Figure 4.1: Particle size distribution curves of synthesized emulsions**

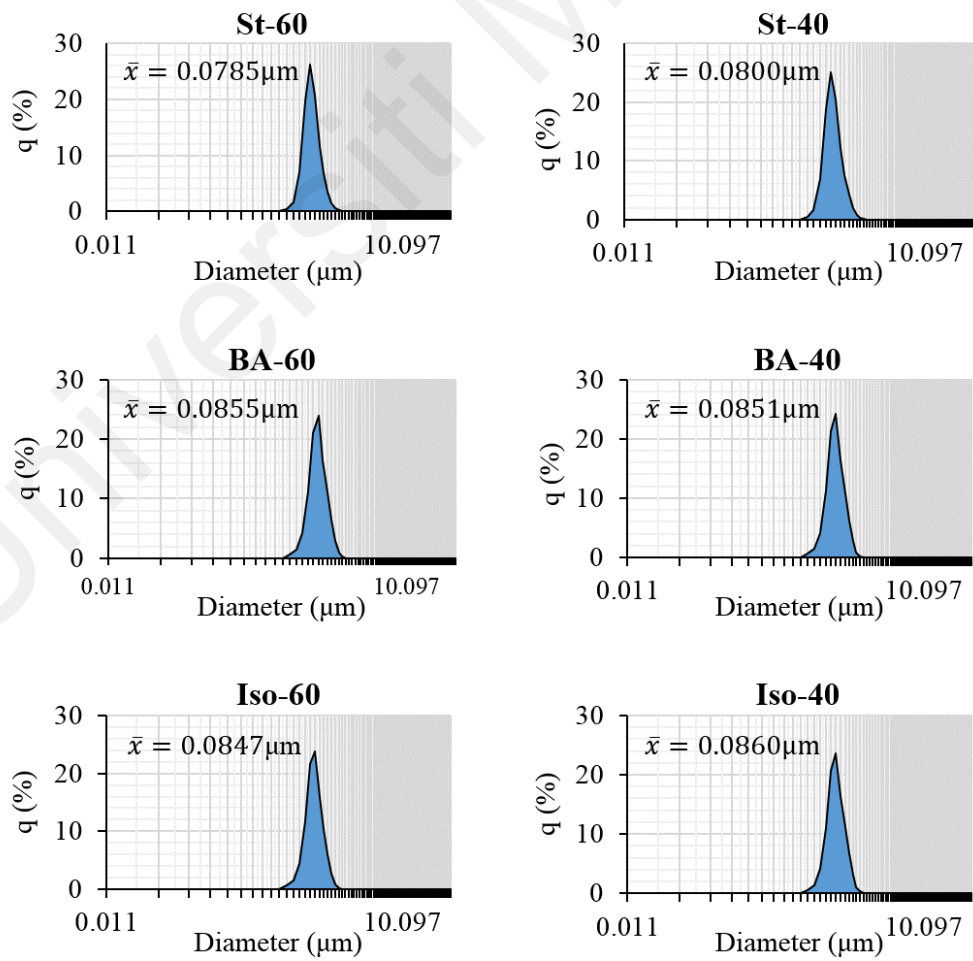


**Figure 4.2: Detailed particle size curves for each emulsion**

Zeta potential is a crucial physicochemical parameter that is used to measure the potential difference between the mobile dispersion medium and the stationary layer of the dispersion medium that attached to the dispersed particle (Lu & Gao, 2010). The magnitude of the zeta potential gives indication of the stability of colloidal dispersion (Selvamani, 2019). This is particularly significant in producing resin for glove coating as it can be related to the short- and long-term stability of the emulsions during storage. In most of the reported study, emulsions with higher zeta potential value of 30 mV to 50 mV (negative or positive) are electrically stabilized due to electrostatic repulsion of individual particles (Joseph & Singhvi, 2019; Shnoudeh et al., 2019). On the contrary, emulsions with lower zeta potential value are generally considered less stable and may lead to particle aggregation, coagulation and flocculation due to Van der Waals attraction between the particles (Shnoudeh et al., 2019).

According to Table 4.2 and Figure 4.3, it is clearly observed that all emulsions reported high zeta potential value which ranges from -35.2 to -55.1 mV, suggesting high colloidal stability possessed by all emulsions. The enhanced stability found could be due to the appropriate amount of surfactant used for the synthesis, in which the additional surface charge provided by the surfactant increased the repulsion potential energy (El-Sherif et al., 2017). However, a detailed look into the zeta distribution curve of each emulsion (Figure 4.4 – 4.9) shows that St-40 has the narrowest unimodal distribution. It is worth to note that zeta potential with narrow distribution and higher magnitude indicates that emulsion has great colloidal stability against coalescence and flocculation. Meanwhile, Iso-60 showed a distinctive bimodal distribution and slightly lower zeta potential (-35.2 mV) than the rest. This could be attributed to lower conversion % which lead to the presence of some unreacted monomers in the emulsions. However, since all emulsion achieved zeta potential higher than -30 mV, it can be deduced that all synthesized emulsions showed good stability.

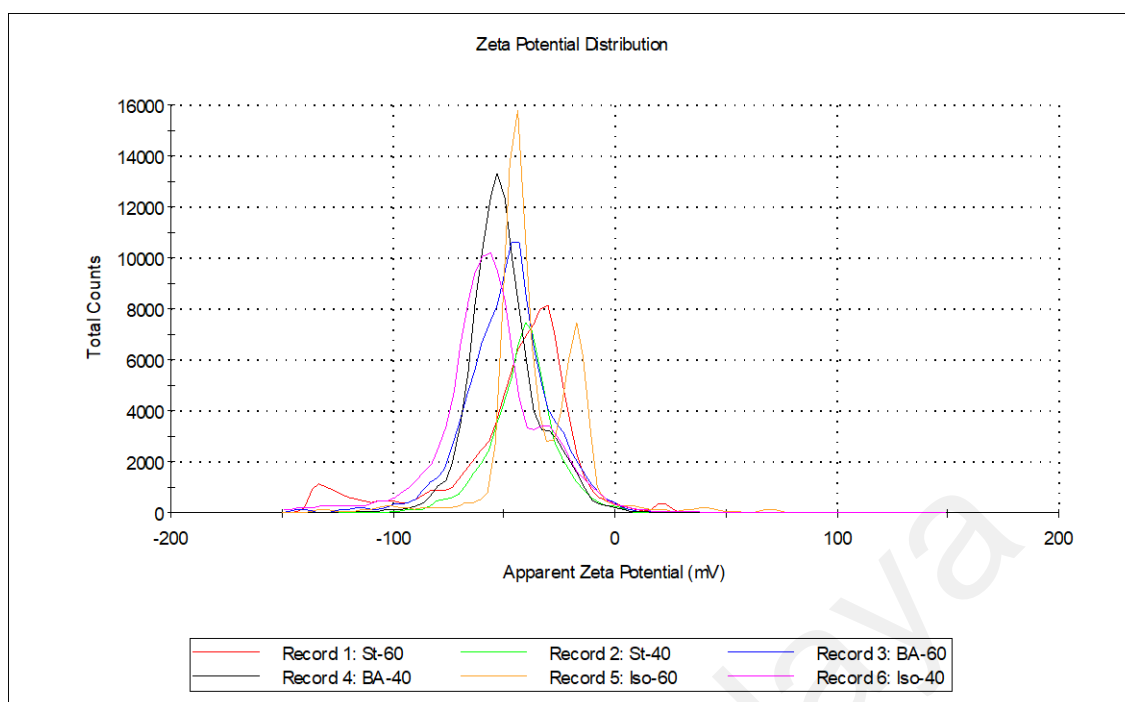


**Figure 4.3: Zeta potential distribution curves of all emulsions**

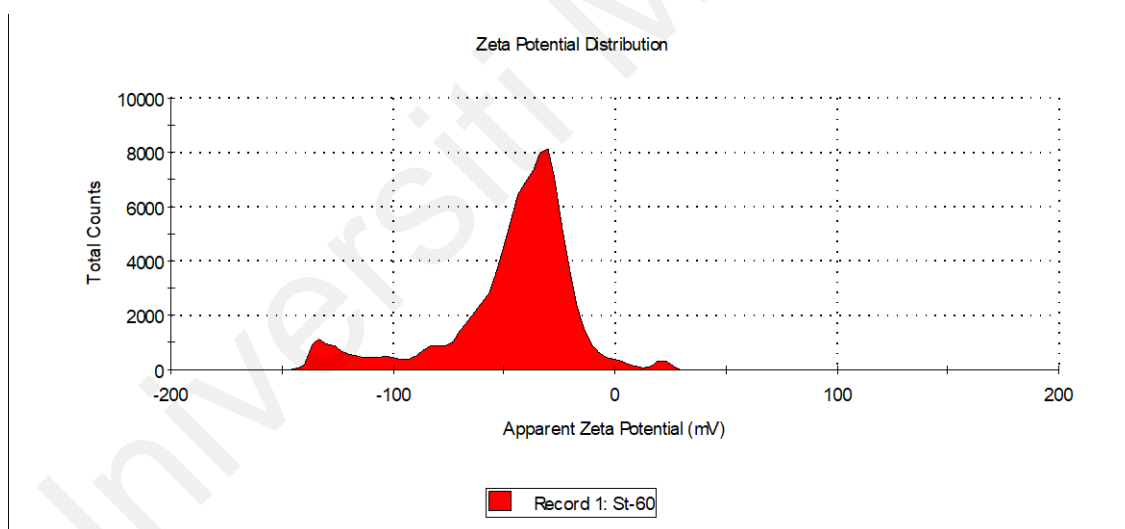


**Figure 4.4: Zeta potential distribution curve for St-60**

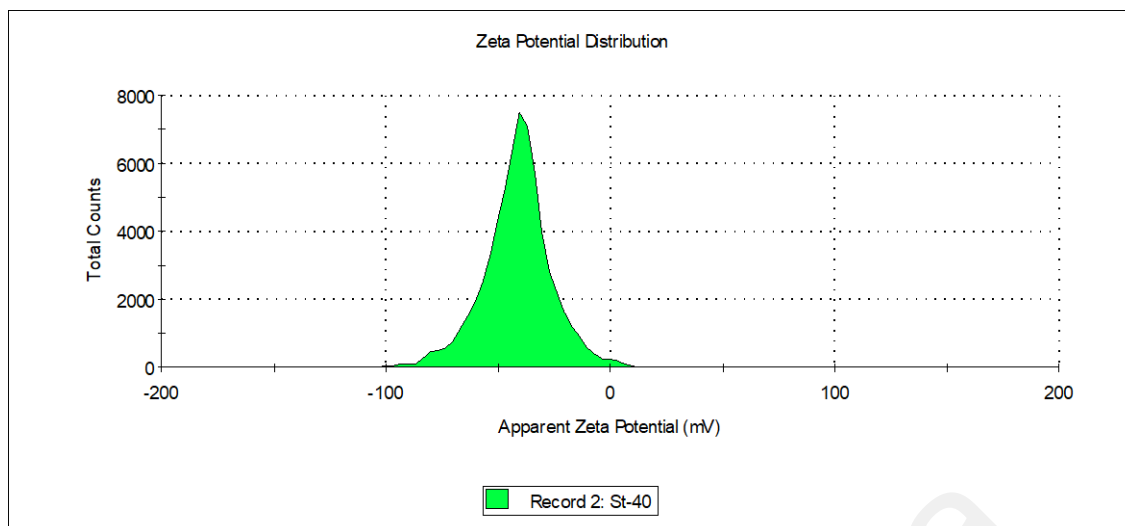


**Figure 4.5: Zeta potential distribution curve of St-40**

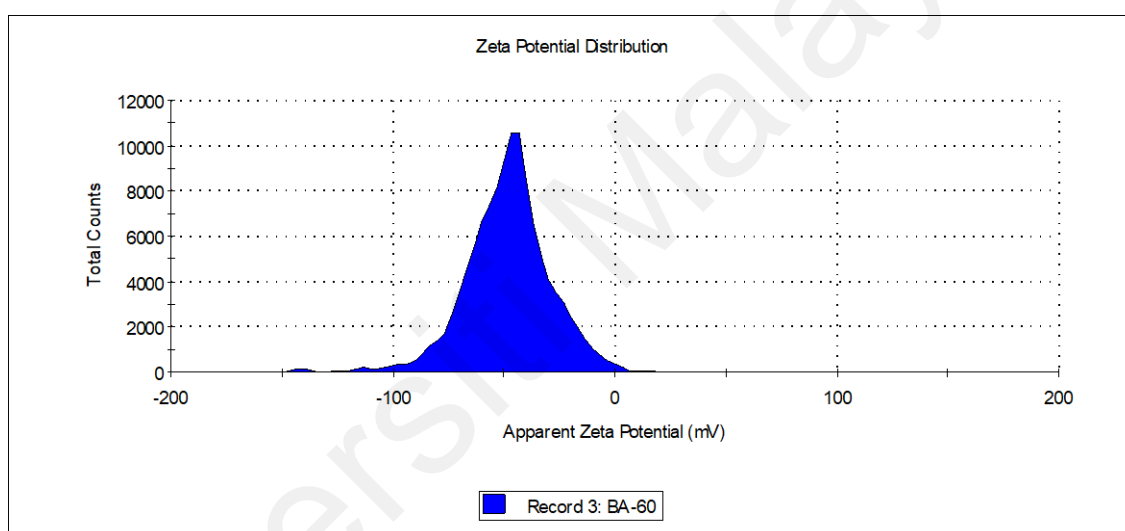


**Figure 4.6: Zeta potential distribution curve of BA-60**

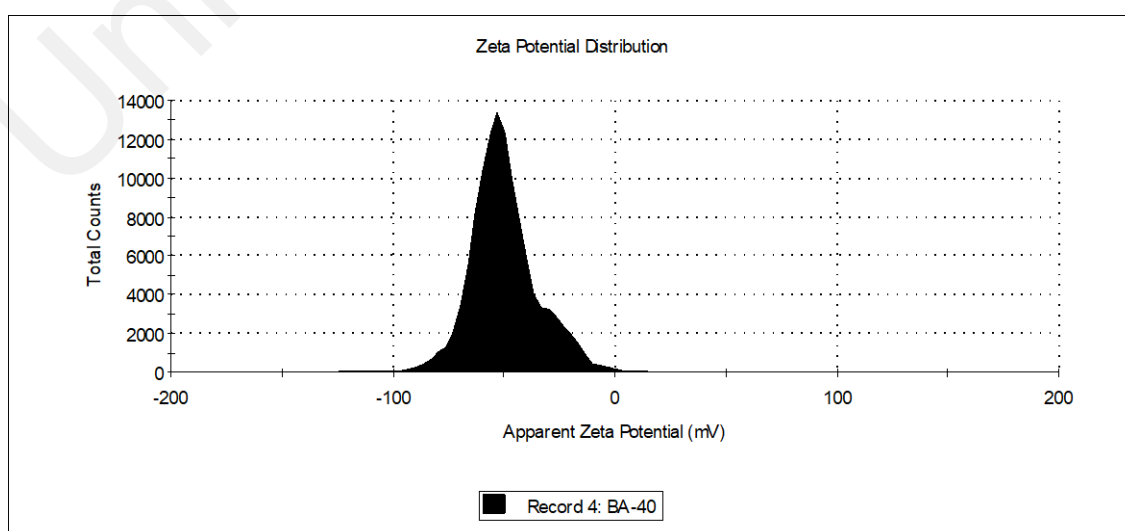


**Figure 4.7: Zeta potential distribution curve of BA-40**

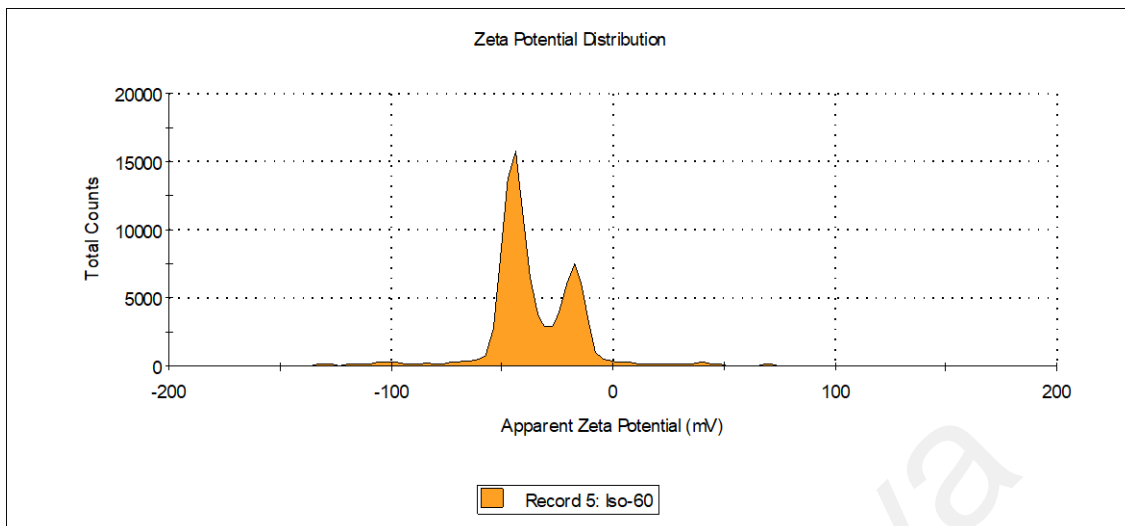


**Figure 4.8: Zeta potential distribution curve of Iso-60**

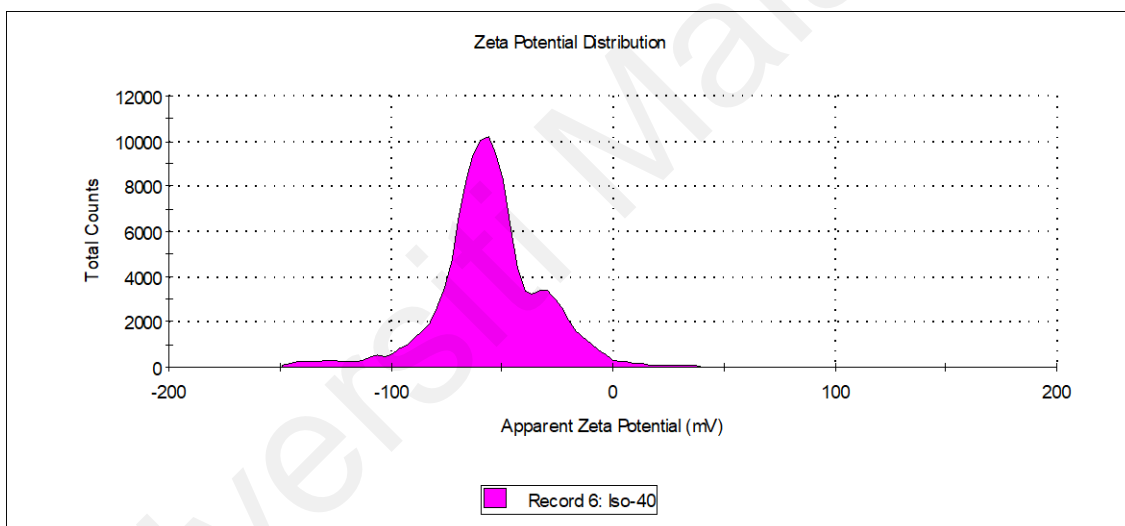


**Figure 4.9: Zeta potential distribution curve of Iso-40**

## 4.2 Characterization of St-BA-Iso copolymer film

### 4.2.1 ATR-FTIR

FTIR analysis was carried out to elucidate the chemical structure of the synthesized copolymer. Figures 4.10 and 4.11 present the FTIR spectra of the monomers used and St-BA-Iso copolymers, respectively. All St-BA-Iso copolymers produced similar FTIR absorption peaks, as shown in Figure 4.11. Absorption peaks in the region 2960 to 2852  $\text{cm}^{-1}$  corresponds to the  $\text{sp}^3$  hybridized  $\text{C-H}$  stretching such as that of stretching vibration

of methylene group  $-CH_2$  within the butyl acrylate segment (Li et al., 2016). Major peaks at  $1730\text{ cm}^{-1}$  and  $1158\text{ cm}^{-1}$  could be ascribed to the carbonyl,  $C=O$  and  $C-O$  groups of butyl acrylate, respectively. Another intense absorption peak at around  $700\text{ cm}^{-1}$  is due to the out of plane bending of aromatic  $-CH$  belongs to styrene. Less intense peak can be observed at around  $3050\text{ cm}^{-1}$  is attributed to  $sp^2$  carbon of styrene (Francisco-Vieira et al., 2019; Sornsanee et al., 2018).

There is a peak with medium intensity observed at  $750\text{ cm}^{-1}$  which can be attributed to the  $-CH_2$  in cis 1,4-polyisoprene unit (Wang et al., 2021). According to FTIR spectrum of isoprene monomer from Figure 4.10, it shows a strong absorption band at  $888\text{ cm}^{-1}$  which is due to the out of plane bending of  $CH_2$  in  $C=CH_2$  (Chen et al., 2013). However, the characteristic peak at  $888\text{ cm}^{-1}$  is no longer visible in all spectra, suggesting that the isoprene has been successfully polymerized in the polymerization process. It is noteworthy that the terminal unsaturation  $C=CH_2$  is only present in isoprene monomer, but not after it has polymerized. Ultimately, the FTIR spectrum reveals that all monomers have participated in the emulsion copolymerization to produce St-BA-Iso emulsion copolymer as desired. The summary of peaks attribution for each monomer and St-BA-Iso copolymer is as tabulated in Table 4.3 and 4.4 respectively.



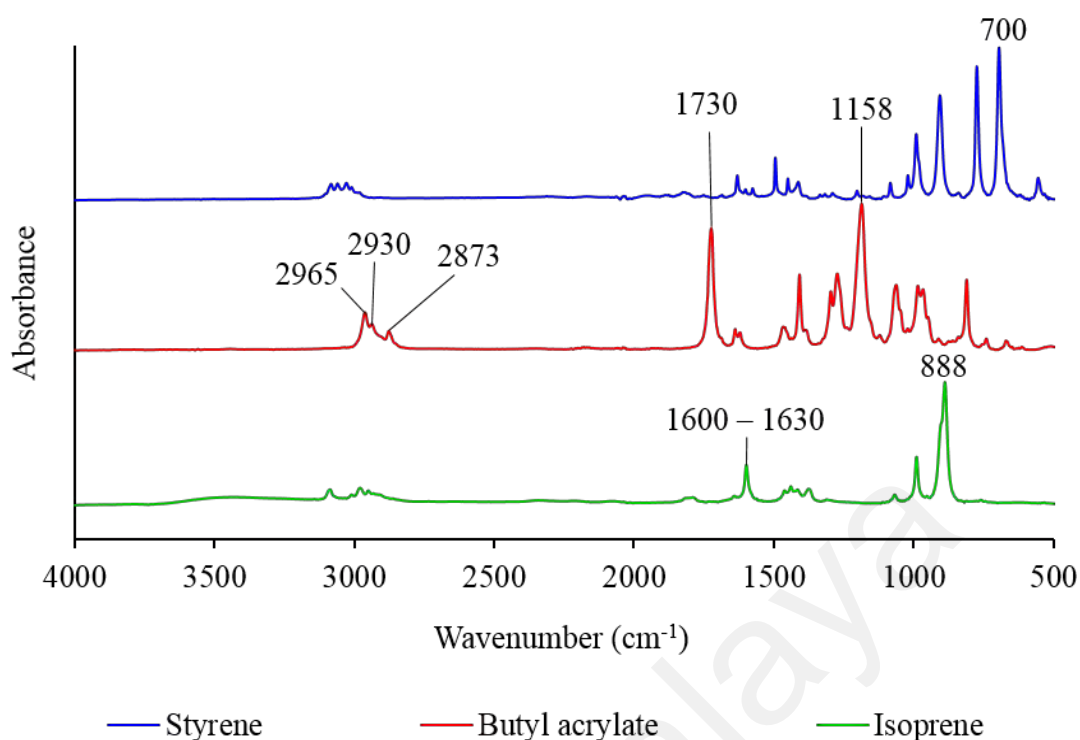


**Figure 4.10: FTIR spectra of St, BA, and Iso monomers**

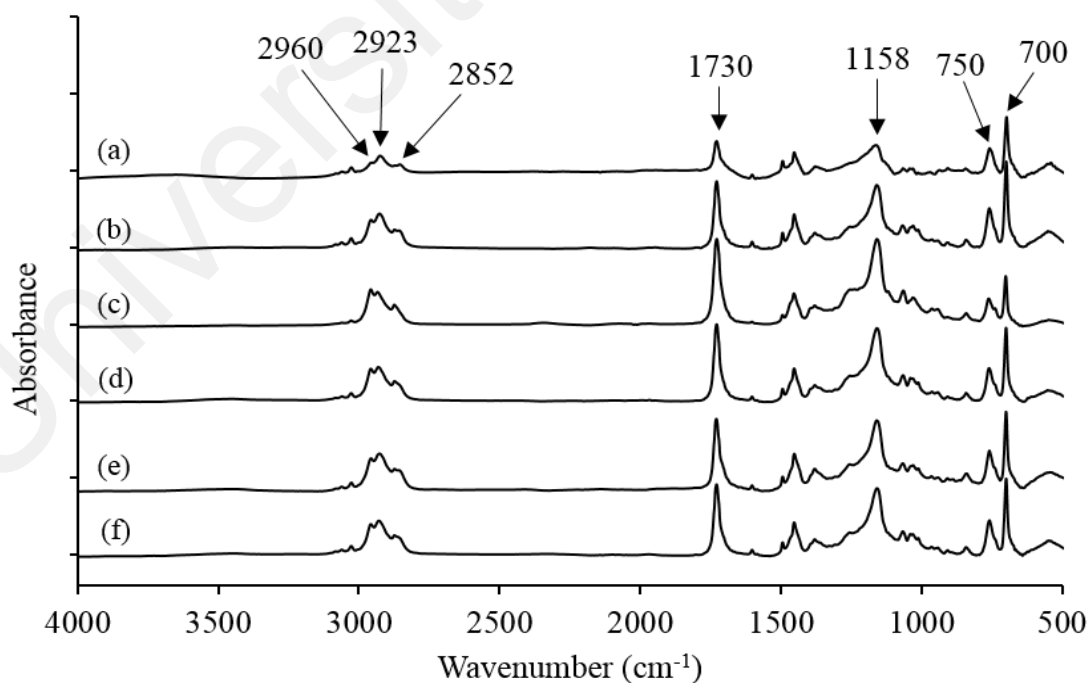


**Figure 4.11: FTIR spectra of (a) St-60, (b) St-40, (c) BA-60, (d) BA-40, (e) Iso-60, (f) Iso-40 copolymers**

**Table 4.3: Assignment of characteristic IR peaks for each monomers**

Monomer	Wavenumber (cm <sup>-1</sup> )	Attribution
Styrene	700	out of plane bending of aromatic $-CH$
Butyl acrylate	2965, 2930	stretching vibration of methyl group $-CH_3$
	2873	stretching vibration of methylene group $-CH_2$
	1730	carbonyl group $C=O$
	1158	ether group $C-O-C$
Isoprene	888	out of plane bending of $CH_2$ in the $C=CH_2$
All	1600 – 1630	Stretching vibration of saturated $C=C$

**Table 4.4: Assignment of characteristic IR peaks for St-BA-Iso copolymers**

Wavenumber (cm <sup>-1</sup> )	Attribution
2960, 2923	$sp^3$ hybridized $C-H$ groups
2852	stretching vibration of methylene group $-CH_2$
1730	carbonyl group $C=O$
1158	ether group $C-O-C$
750	$-CH_2$ stretching in cis 1,4-polyisoprene unit
700	out of plane bending of aromatic $-CH$

#### 4.2.2 <sup>1</sup>H-NMR

The chemical structure and composition of the synthesized copolymers were determined by proton nuclear magnetic resonance (<sup>1</sup>H-NMR) spectroscopy and the spectrum of the optimum sample (St-40) is shown in Figure 4.12. The chemical shifts of <sup>1</sup>H-NMR were calibrated with tetramethylsilane (TMS) as internal standard to lock the signal at  $\delta = 0$  ppm, and CDCl<sub>3</sub> at  $\delta = 7.26$  ppm. From the figure, a broad peak which resonates at around 7.10 ppm can be assigned to the aromatic protons of styrene, H<sub>a</sub> (Francisco-Vieira et al., 2019). These aromatic protons are deshielded far downfield by the large anisotropic effect generated by the electrons in the ring's  $\pi$  system. Next, the

peak at about 4.80 ppm is mainly attributed to  $H-C=C$ - proton,  $H_b$  of the isoprene repeating unit (Tumnantong et al., 2017). The deshielding of the vinyl hydrogen is mainly due to the anisotropic effect caused by the  $\pi$  electrons in the adjacent double bond. The chemical shift at 3.44 ppm corresponds to the methylene protons  $H_c$  on the carbon attached to the single bonded oxygen of the adjacent ester linkage  $COO$ - of BA, and the protons are deshielded due to the electronegativity of oxygen (Hua & Dubé, 2011).

On the other hand, the most shielded protons are the methyl group protons belong to BA repeating unit which resonates at around 0.80 ppm. Other peaks at around 1.30 to 2.10 ppm are attributed to the remaining methyl and methylene protons in the copolymer (Ríos-Osuna et al., 2016). Taking into consideration that the % of conversion is as high as 95 %, and unique peaks that corresponds to each monomer are present in the spectrum of the copolymer, it can be reasonably deduced that the copolymerization involving the three monomers was successful. The summarized peak assignments are as listed in Table 4.5.

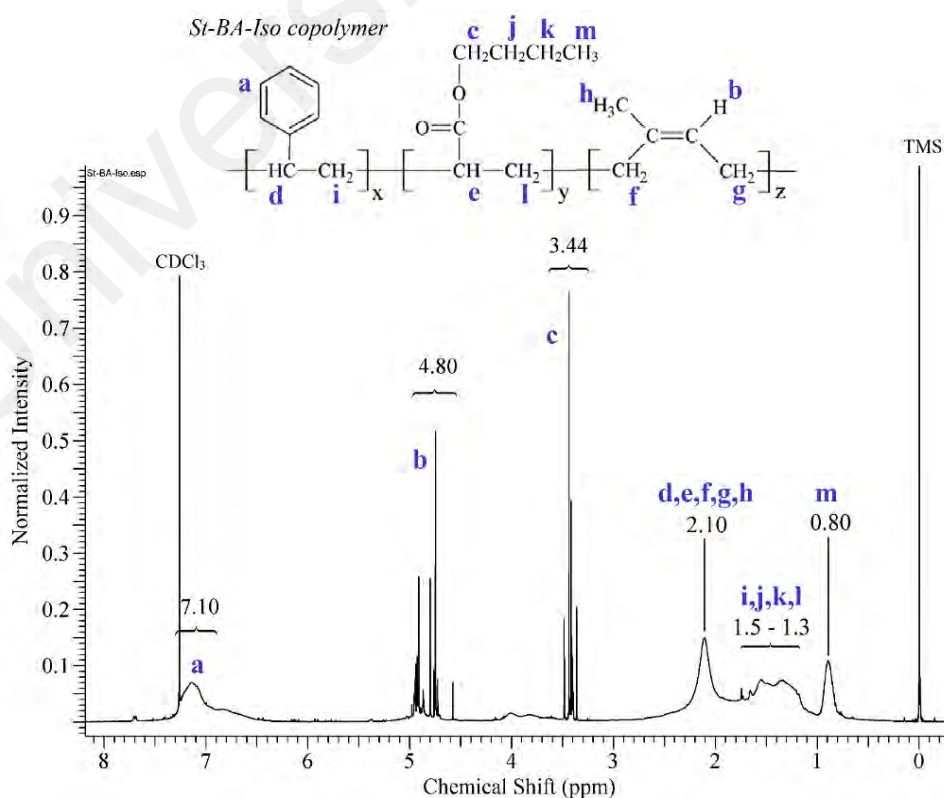


**Figure 4.12:  $^1H$ -NMR spectrum of the St-40 copolymer**

**Table 4.5: Attribution and chemical shifts of St-40 from  $^1\text{H}$ -NMR analysis**

Peak	Chemical shift (ppm)	Attribution
a	7.10	aromatic protons of styrene
b	4.80	$H-C=C$ - proton of isoprene repeating unit
c	3.44	methylene protons adjacent to the ester linkage of BA, $-COO-CH_2-$
d – h	2.10	methyl and methylene protons adjacent to benzene ring, ester linkage of BA, or $C=C$ of isoprene unit
i – l	1.50 – 1.30	remaining methylene protons
m	0.90	methyl proton of BA repeating unit and chain terminal

#### 4.2.3 TGA

Thermal analysis of polymers provides information about their properties and thermal stability, which is also particularly crucial in determining materials' suitability for the intended usage, and in this case, it reflects the suitability of the polymer coating to be handled at elevated temperature during gloves' making and processing. Thermal analysis using TGA was performed on the dried film of the copolymers to assess the thermal behaviour of the copolymer films made of different monomers composition. The obtained thermograms are summarized in Figure 4.13.

A minimal weight loss observed around 100 °C in some of the samples are due to the evaporation of trapped moisture in the samples. At temperature above 300 °C, all samples start to exhibit apparent degradation weight loss. As the heating temperature further increased, the degradation rate for all samples increased constantly until the temperature reached around 455 °C. The total weight loss up to this period is approximately 92 % for all samples. A detailed look into the first derivative curve depicted in Figure 4.14 shows that the peak temperature that corresponds to the maximum rate of weight loss ( $T_p$ ) of all samples are similar and took place at temperature above 400 °C.

To sum up, similar trend in thermal behaviour were observed in all samples which showed reasonably good thermal stability, and it can be deduced that different composition of monomers used to synthesize the copolymers have no major influence on its thermal stability. On top of that, as detailed earlier in the methodology, the processing temperatures such as the curing, leaching, and drying of the coated rubber articles are usually well under 200 °C. Therefore, the copolymer coating which exhibit onset of degradation at temperature above 300 °C is considered sufficiently high for rubber glove or other elastomeric coating applications.

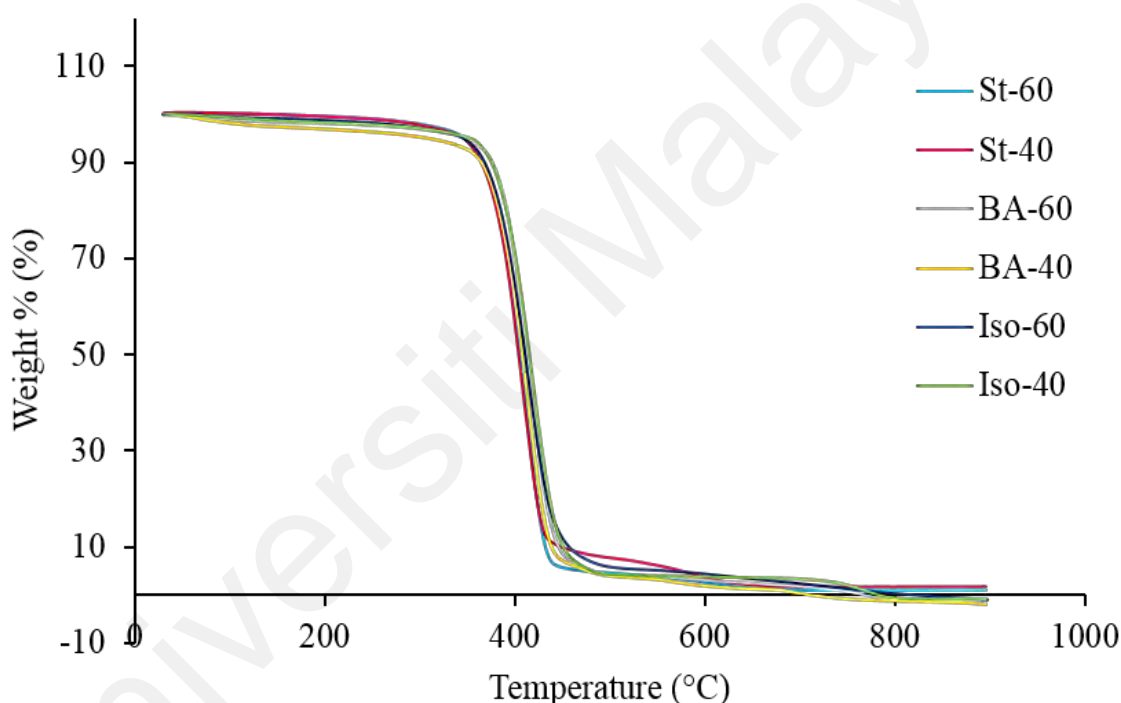


**Figure 4.13: TGA thermograms of St-BA-Iso copolymers**

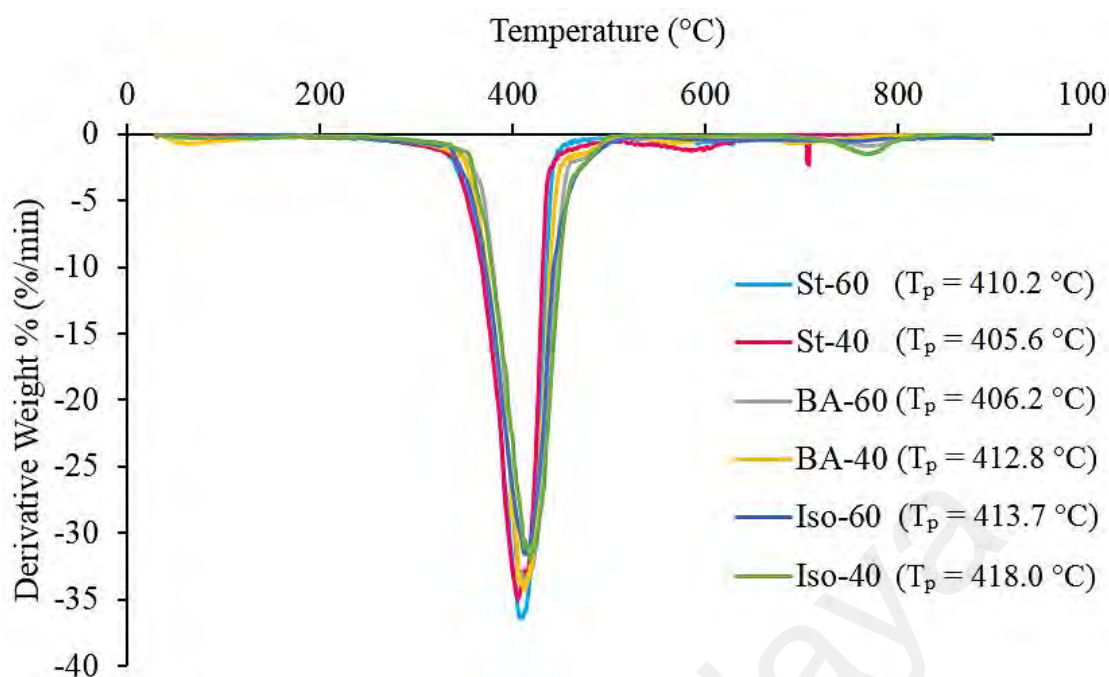


**Figure 4.14: First derivative TGA thermograms of St-BA-Iso copolymers**

#### 4.2.4 DSC

Glass transition temperature, often referred as  $T_g$ , is the temperature at which there is a change in the molecular mobility of a material which often causes substantial changes in its properties (Campo, 2008). Below the  $T_g$ , the amorphous polymer tends to be hard and glassy due to relatively little mobility of the polymer molecules. Above  $T_g$ , they become soft and have higher elasticity, behaving like rubbery materials (Ebnesajjad, 2016). The  $T_g$  of the homopolymers produced from the monomers involved in the synthesis of the copolymer is as listed in Table 3.1 in the previous chapter. Based on the  $T_g$  values, St can be classified as hard monomer, while BA and Iso are considered as soft monomers. For polymer coating application, the determination of  $T_g$  is a very important aspect as the  $T_g$  values affect the coating film properties such as surface tackiness and coating adhesion. DSC was used to analyse the  $T_g$  of St-BA-Iso copolymers. The obtained  $T_g$  values for all sets are tabulated in Table 4.6 and the DSC thermograms obtained are shown in Figure 4.15.

As expected, St-60 copolymer which comprised of the highest proportion of styrene in all formulations recorded the highest  $T_g$  at 45.4 °C, followed by St-40 copolymer with  $T_g$  of 24.0 °C. At ambient temperature, both copolymers exhibit glassy condition, contributing to the smoothness of the film produced. However, between the two, St-60 film appears to be harder and brittle, causing the film to crack easily. This could be attributed to the presence of excessive amount of aromatic rings in the system which restrict the flexibility and freedom of motion of the polymer chains, and this explains the relatively rigid film observed in St-60 (Saha & Bhowmick, 2019).

Iso-60 copolymer with the highest loading of isoprene recorded the lowest  $T_g$  of -16.7 °C, followed by BA-60 copolymer with  $T_g$  of 3.0 °C. This is because the  $T_g$  of the film reduced with the increase in the proportion of soft monomers, producing films which are more rubbery and sticky. On the other hand, the  $T_g$  of Iso-40 and BA-40 do not differ much since the difference in the amount of Iso: BA used in both formulations is relatively small. In the context of rubber glove coating application, the copolymer with the most preferable  $T_g$  would be St-40, as it depicted moderately high  $T_g$  of 24 °C. The temperature is very much like the ambient temperature, indicating that the coating may be glassy during use but is not too stiff to enable adequate adhesion to the rubber substrate.

**Table 4.6: Glass transition temperature ( $T_g$ ) of St-BA-Iso terpolymer films**

Sample	$T_g$ obtained (°C)
St-60	45.4
St-40	24.0
BA-60	3.0
BA-40	8.9
Iso-60	-16.7
Iso-40	14.5

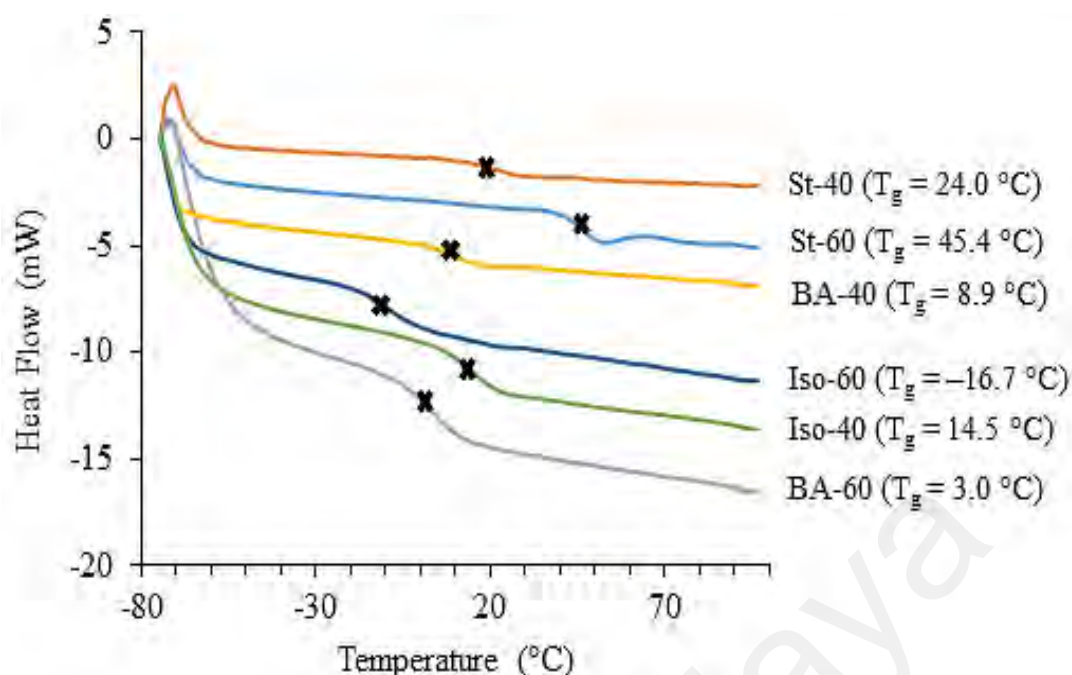


**Figure 4.15: DSC thermograms of St-BA-Iso terpolymer films**

#### 4.2.5 Tensile test

Tensile strength is the maximum tensile stress applied to a specimen until it ruptures while ultimate elongation at break is the percentage change in the length of a specimen prior to rupture. Tensile testing was conducted on the copolymer film samples, as well as the uncoated rubber film which acts as the control to evaluate their films stiffness and extent of elongation. Nevertheless, it is worth to note that the tensile strength of the copolymer film itself is not of a major concern as it will be coated on the rubber substrate.

Summary of the mechanical test properties are shown in Table 4.7 and Figure 4.16. As predicted, St-60 with highest T<sub>g</sub> exhibited lowest elongation at break due to its high degree of stiffness. The brittleness of the sample also makes it difficult to determine its accurate tensile strength, where most of the samples fractured right away in the beginning of the test. On the contrary, BA-60 which constituted of higher loading of soft monomer butyl acrylate reported the lowest tensile strength and highest elongation at break, closest to that of natural rubber film. This indicates that BA-60 possesses comparable film



flexibility as the rubber film and is expected to demonstrate excellent adhesion and minimal flaking from the rubber substrate upon stretching.

As for Iso-60 and Iso-40, although they too were synthesized with high proportion of soft monomer, isoprene, the copolymers exhibited relatively higher tensile strength and lower elongation % as compared to BA-60 and BA-40, respectively. This could be attributed to increased crosslinking between the polymer chains involving the double bonds from the isoprene moiety in the polymer. The crosslinking has restricted the elongation of the film and increased the strength of the copolymer (Blanchard et al., 2020; Nuzaimah et al., 2021).

Copolymer film with the highest tensile strength and reasonably closest to that of rubber film is St-40. Although its elongation at break is slightly lower than the rest, it is partially compensated with a higher tensile strength where greater stress is needed to break the polymer film, and this has indirectly reduced the chances of cracking or delamination to happen, as proven from the water turbidity test (Figure 4.17 (b)) and SEM images (Figure 4.18) shown in later discussion.

**Table 4.7: Mechanical test outcomes for St-BA-Iso copolymers**

Samples	Tensile Strength (MPa)	Elongation (mm)	Elongation (%)
Uncoated rubber film	25.72	432.38	2161.88
St-60	0.97	15.09	75.43
St-40	5.04 ± 0.43	260.90	1304.47
BA-60	0.17 ± 0.02	476.93	2384.64
BA-40	1.23 ± 0.36	352.39	1761.93
Iso-60	2.19 ± 0.42	357.39	1786.93
Iso-40	1.67 ± 0.23	351.13	1755.66

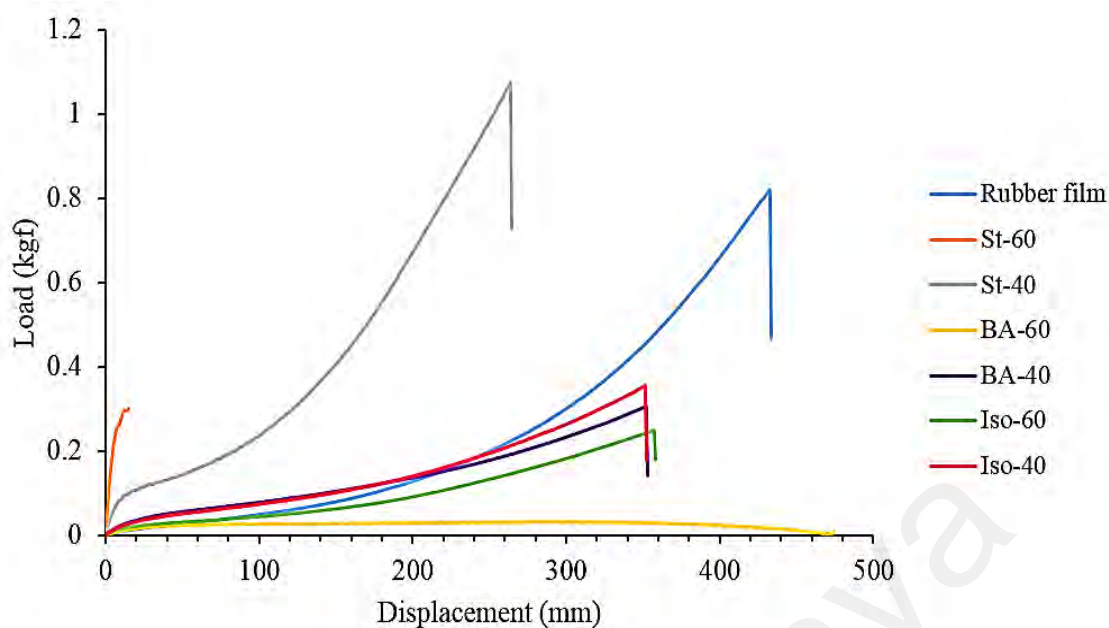


**Figure 4.16: Force-displacement curves of St-BA-Iso copolymer films**

### 4.3 Coating performance on rubber substrate

The types and ratio of monomer used have significant impact on the properties of the synthesized emulsion. Various monomers are selected through formula design to fulfil the requirement of surface smoothness, film flexibility, excellent adhesion to the substrate, as well as resistance to high temperature. The types and functions of monomers used in this study are listed in Table 4.8.

**Table 4.8: T<sub>g</sub> of homopolymers and its functions**

Monomer	T <sub>g</sub> of homopolymer (°C)	Function
St	100	Hard segment, gloss, surface smoothness, water resistance, pollution resistance
BA	-54	Soft segment, film flexibility, adhesive, water resistance
Iso	-61	Soft segment, film softness, adhesive
AA	106	Functional monomer, emulsion stability

(Zhang et al., 2017)

The three main monomers used in this study are St, BA and Iso. Other than contributing to the film glossiness and surface smoothness, St also increases the resin's resistance to pollution, at the same time reducing the cost (Zhang et al., 2017). Meanwhile, both BA and Iso are soft and tacky by nature, providing good tack and peel strength. In addition to the main monomers, a very little amount of acid-functional monomer, AA was added in this formulation. The repulsive negative charges on the surfaces of emulsion particle help to enhance the colloidal stability (Tan et al., 2016).

#### 4.3.1 Coefficient of friction

Coefficient of friction (CoF) test was performed on coated rubber films and the values reflect the surface smoothness and level of difficulty in donning such coated rubber gloves. Table 4.9 shows kinetic CoF values of the coated rubber films, as well as those of uncoated rubber film to serve as control. Evidently, uncoated rubber film has the highest CoF value due to its inherent tacky surface, and glove produced from such film will be difficult to don and is uncomfortable to wear for long period of time. Rubber film coated with St-60 copolymer displayed the lowest CoF value (0.079), followed by St-40 coating (0.098). The result is consistent with their high  $T_g$ , in which the films are hard and smooth with the increase in the proportion of styrene in the formulation.

Unsurprisingly, coating that showed the highest CoF is also the one with the lowest  $T_g$ , Iso-60. The coated film is very tacky, and generates strong friction during the sliding process, implying that it will be much more difficult to don such glove. BA-60 coating also recorded relatively high CoF value of 0.246, and collectively the results suggest that formulation with higher content of soft monomers such as Iso and BA could lead to formation of more tacky film. From the CoF analysis, St-60 and St-40 coatings outperformed the rest in terms of film smoothness and ease of donning as evidenced by their significantly lower CoF value.

**Table 4.9: Kinetic CoF values for uncoated rubber films and rubber films coated with St-BA-Iso copolymers**

Samples	Kinetic CoF
Uncoated rubber film	1.222
St-60	0.079
St-40	0.098
BA-60	0.246
BA-40	0.168
Iso-60	0.307
Iso-40	0.126

#### **4.3.2 Visual evaluation on polymer coated rubber film**

Physical evaluation was also carried out by rubbing the donning surfaces together with pressure, using thumb and index finger to check for the tackiness of the coats. The outcome was in good agreement with the CoF value reported, in which St-60, St-40 and Iso-40 produced non-tacky films, meanwhile the rest of films are tacky. Similar outcome was observed in the blocking test, with St-60, St-40 and Iso-40 coatings not adversely affected upon being conditioned for blocking test. On the contrary, the other coatings showed stickiness and the donning surface stick to each other. The significance of blocking test is to determine whether the donning side of gloves stick together when exposed to higher surrounding temperature during shipping and packaging. Hence, glove that exhibits good anti-blocking property is expected to be glove of high quality. The outcome of the visual examination on all samples was tabulated in Table 4.10.

**Table 4.10: Film tackiness inspection and outcomes from blocking test**

Samples	Film tackiness	Blocking test (70 °C for 24 h)
Uncoated rubber film	Very tacky	Very sticky
St-60	Non-tacky	Non-sticky
St-40	Non-tacky	Non-sticky
BA-60	Tacky	Internal stickiness
BA-40	Tacky	Internal stickiness
Iso-60	Tacky	Internal stickiness
Iso-40	Tacky	Internal stickiness

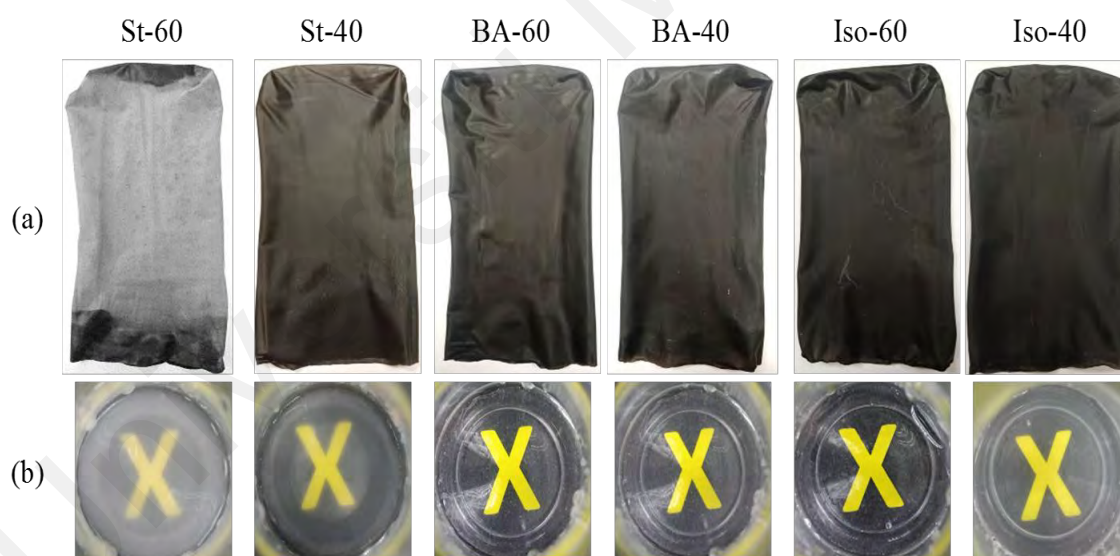
Polymeric coating with poor adhesion on rubber substrate often experience surface defects such as cracking or delamination, especially after the coated articles were stretched. To examine the extent of flaking/ delamination of the polymeric coating, a visual inspection was carried out by stretching the coated rubber films to the maximum before releasing and conditioning them at room temperature (Yeh & Zhu, 2002).

Figure 4.17 (a) shows the appearance of the coated rubber film after it was stretched while Figure 4.17 (b) shows the clarity of water that was used to soak the stretched coated rubber during the water turbidity test. Rubber film coated with St-60 exhibited the most prominent white patch formation upon stretching and the most turbid water, implying that the coated St-60 polymeric layer delaminates easily from the rubber surface. This is not unexpected after considering the highest  $T_g$  and lowest CoF value depicted by the St-60 copolymer which has led to hard and brittle film.

Meanwhile, on the St-40 coating, there was significantly less visible white patch formed, and water from the rubbing test is only mildly turbid. Reducing the proportion of hard monomer, styrene from 60 to 40 % managed to significantly improve the

delamination issue. In contrast, rubber film coated with Iso-60 and BA-60 emulsion which constituted of the highest ratio of soft monomers, isoprene and butyl acrylate respectively, did not show any severe white patch formation and the X-mark from the water turbidity test remain highly visible. The outcome is consistent with the low  $T_g$  reported, high CoF, and high tackiness of the film that has resulted in good adhesion property and lesser tendency to crack. Moreover, the outcome is also further supported with having high elongation to break proven by the tensile test result as discussed earlier.

In spite of possessing superior film adhesion and lesser flakiness, rubber films coated with BA-60, BA-40, Iso-60 and Iso-40 copolymers exhibited relatively high tackiness and CoF value, hence it has drawn up an agreement that they are not the best candidate to serve as polymeric coating for smooth gloves donning.



**Figure 4.17: (a) White patch appearance of films after stretched and (b) water cloudiness from water turbidity test**

### 4.3.3 SEM analysis

For a closer examination on the extent of coating flakiness or delamination, the surface morphology of the polymer coated rubber films were inspected using SEM at greater magnification and higher resolution. Figure 4.18 shows the SEM images of copolymer

coated rubber films after they were stretched. The captured SEM images are consistent with the severity of white patch observed in Figure 4.17 (a), in which rubber film coated with St-60 showed the most severe flakiness and delamination, while the rest of the coatings did not show any substantial flaking. Apart from that, the outcomes were also in good agreement with the tensile test results presented earlier, in which the poorly adhered St-60 coating showed extensive delamination and flaking upon stretching, hence resulted the lowest elongation to break. Meanwhile, higher elongation % for the rest of the copolymer films also were proven by less severe coating delamination.

To summarize, all of the above-mentioned findings manifested that St-40 would be the finest candidate, as it demonstrated a more balanced properties by having moderate  $T_g$  with low CoF value, and at the same time did not show any significant cracking/delamination upon stretching or during water turbidity test. A fine-tuned ratio of hard and soft monomers used to synthesize the emulsion could have led to the balanced desired film property. The findings from this work have demonstrated the need to control the feed ratio of monomers used for the synthesis of St-BA-Iso copolymer in order to produce polymeric resin with good film properties for rubber glove coating application.



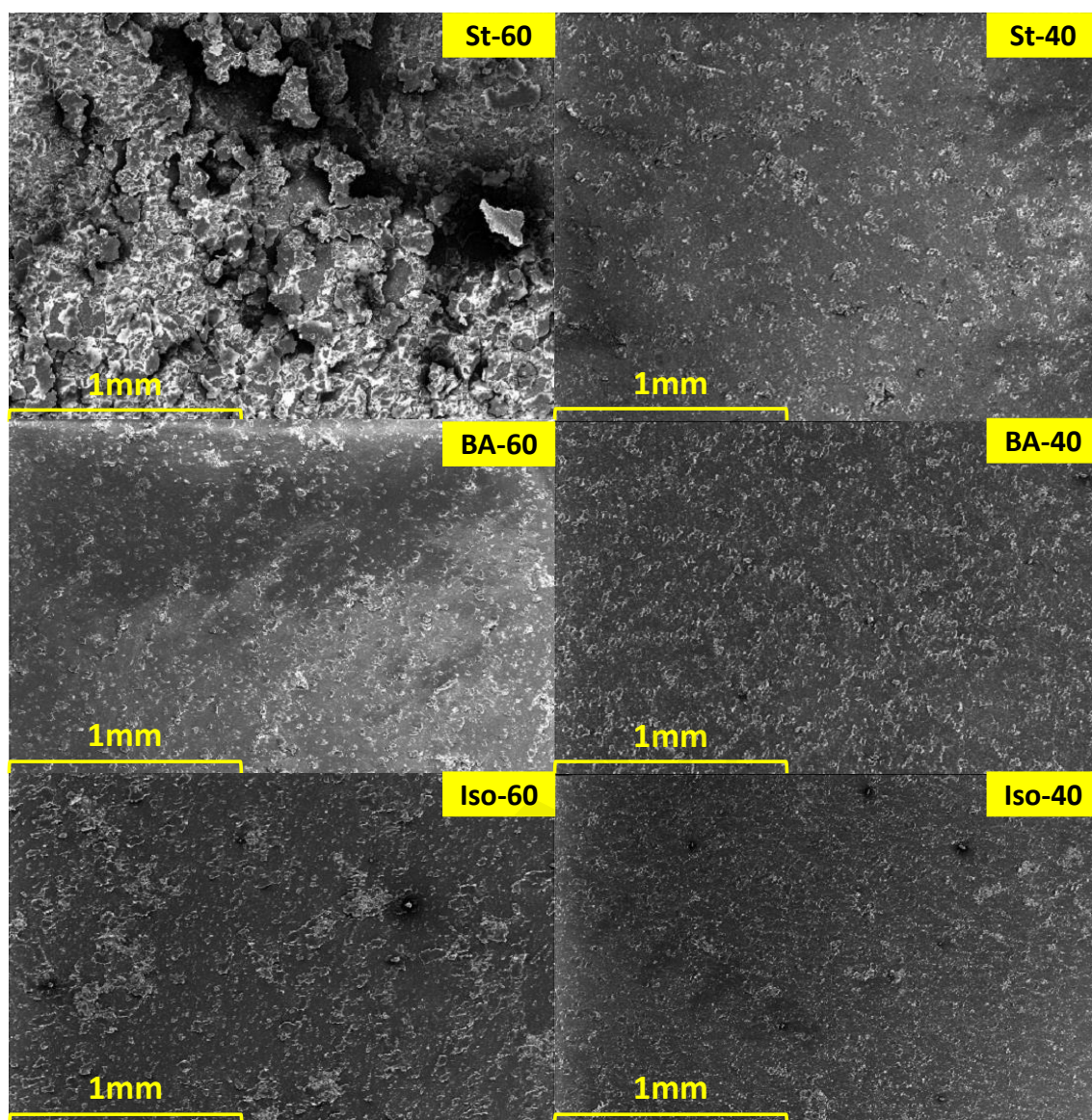


Figure 4.18: Stretched rubber films coated with St-BA-Iso copolymer



## CHAPTER 5 : CONCLUSION

### 5.1 Summary

In summary, a series of St-BA-Iso emulsion copolymer constituted of three main monomers (i) styrene, (ii) butyl acrylate and (iii) isoprene has been synthesized by varying the monomers composition. The synthesis involved seeded emulsion polymerization which was carried out in a temperature-controlled water bath system at  $70 \pm 2$  °C, in addition with other components including surfactant, initiator, activator and water. All the synthesized emulsions appeared as milky white emulsion, and mostly achieved the targeted conversion % and solid content. Further characterization to elucidate the structure of the synthesized St-BA-Iso copolymer was carried out using ATR-FTIR and  $^1\text{H}$ -NMR. The spectra obtained showed a combination of all characteristic peaks of the three main monomers involved, justifying that the St-BA-Iso copolymers were successfully synthesized. In addition, zeta potential and surface tension analysis showed that the emulsions have good stability, proven by small particle mean size in the range of  $82 \pm 4$  nm, and zeta potential well above -30 mV.

Thermal analysis revealed that all emulsions showed comparable thermal stability, with apparently high decomposition temperature well above 400 °C. Apart from that, St-40 showed high tensile strength and acceptable extent of elongation and was comparable to the NR rubber substrate itself. In terms of coating's surface smoothness, results from this study showed that St-40 is the most preferred emulsion copolymer. This is proven when St-40 coating showed moderate glass transition temperature and significantly low coefficient of friction value of less than 0.1. In terms of coating adhesion, emulsion copolymer with higher composition of isoprene and butyl acrylate performed better, however, the coated films surface exhibited high stickiness and/or tackiness due to relatively low glass transition temperature, making them unsuitable for rubber gloves coating application. Meanwhile, St-40 coating appeared to have good coating adhesion,

proven from the very minimal or negligible cracking observed on the coating surface when the rubber film was stretched with maximum force.

As a conclusion, St-40 emulsion copolymer which composed of 40:30:30 weight ratio of St:BA:Iso demonstrated efficient donning property, good anti-blocking, excellent coating adhesion and remarkable mechanical properties. Emulsions with different combinations of hard and soft segments provide diversity and performance, as the hard styrene contributed surface smoothness and enhanced mechanical strength, while the soft butyl acrylate and isoprene promotes adhesion and flexibility of the coatings. Thus, it is crucial to fine tune the ratio of hard to soft monomers in the formulation to produce polymeric coating of balanced and outstanding film properties for rubber gloves coating application.

## **5.2 Suggestions for future work**

This research study proved that the synthesized novel St-BA-Iso copolymer emulsion has a great potential to be used as polymeric coating in gloves coating industry. However, further work extension may be carried out in order to study in depth and develop polymeric coating with enhanced physical and coating properties. This is due to the fact that the characteristics exhibited by these emulsion polymers are mainly determined by the chemical composition of the polymer and the parameters/conditions of the process involved. The nature of emulsion polymers is referred to as “products by process”, which denotes that the main properties of latex are determined during the polymerization process itself (Kim et al., 2022; Tan et al., 2016). The proposed future works would be fabricating a core-shell polymers (CSPs).

CSPs are basically synthesized into a polymer particle which involved a two-stage emulsion polymerization process. The first stage produces nano- and micro-sized latex

cores, while the second stage forms the shell by a continuous addition process. In surface coatings context, CSPs offer various advantages owing to their structural characteristics. It can be employed to produce coatings of desired mechanical properties (such as surface hardness and tensile strength), material functions (such as wettability, surface hydrophobicity/hydrophilicity, enhanced adhesion and friction properties), thermal properties and modified surface texture. For instance, Lu et al. improved the mechanical properties of coated surfaces by using CSP particles with different T<sub>g</sub> values (Lu et al., 1996). In addition, recent study conducted by Kim et al. revealed that coated surface with CSPs showed excellent roughness, favourable hydrophobicity and good wettability on the glass substrate (Kim et al., 2022). Hence, it would be great if further study can be conducted to produce surface coatings fabricated from CSPs in gloves coating application as it may benefit from the synergistic interaction between the core and shell segments, improving the coating performance on the gloves.

## REFERENCES

- Ab Rahman, M. F., Rusli, A., Misman, M. A., & Rashid, A. A. (2020). Biodegradable gloves for waste management post-COVID-19 outbreak: a shelf-life prediction. *ACS Omega*, 5(46), 30329-30335.
- Akabane, T. (2016). Production method & market trend of rubber gloves. *International Polymer Science and Technology*, 43(5), 45-50.
- Ansell, C. W., Medcalf, N., & Williams, P. W. (1993). Gloves. In: Google Patents.
- Askari, F., Nafisi, S., Omidian, H., & Hashemi, S. (1993). Synthesis and characterization of acrylic-based superabsorbents. *Journal of Applied Polymer Science*, 50(10), 1851-1855.
- Asua, J. M. (2004). Emulsion polymerization: From fundamental mechanisms to process developments. *Journal of Polymer Science Part A: Polymer Chemistry*, 42(5), 1025-1041.
- Bassett, D. R., & Hamielec, A. E. (1981). *Emulsion polymers and emulsion polymerization*: American Chemical Society.
- Blanchard, R., Ogunsona, E. O., Hojabr, S., Berry, R., & Mekonnen, T. H. (2020). Synergistic cross-linking and reinforcing enhancement of rubber latex with cellulose nanocrystals for glove applications. *ACS Applied Polymer Materials*, 2(2), 887-898.
- Camacho-Cruz, L. A., Velazco-Medel, M. A., & Bucio, E. (2020). Aqueous polymerizations. In *Green Sustainable Process for Chemical and Environmental Engineering and Science* (pp. 275-318): Elsevier.
- Campo, E. A. (2008). Thermal properties of polymeric materials. *Selection of Polymeric Materials*, 103-140.
- Chen, D., Shao, H., Yao, W., & Huang, B. (2013). Fourier transform infrared spectral analysis of polyisoprene of a different microstructure. *International Journal of Polymer Science*, 2013.
- Chen, S. F., Wang, S., Wong, W. C., & Chong, C. S. (2012). Glove coating and manufacturing process. In: Google Patents.
- Chen, S. F., Wang, S., Wong, W. C., & Chong, C. S. (2015). Glove coating and manufacturing process. In: Google Patents.

- Chern, C. (2006). Emulsion polymerization mechanisms and kinetics. *Progress in Polymer Science*, 31(5), 443-486.
- Cui, X., Mao, S., Liu, M., Yuan, H., & Du, Y. (2008). Mechanism of surfactant micelle formation. *Langmuir*, 24(19), 10771-10775.
- Danková, M., Kalendová, A., & Machotová, J. (2020). Waterborne coatings based on acrylic latex containing nanostructured ZnO as an active additive. *Journal of Coatings Technology and Research*, 17(2), 517-529.
- Davis, E. (1994). Polymer coated contact surface. In: Google Patents.
- de FA Mariz, I., Millichamp, I. S., José, C., & Leiza, J. R. (2010). High performance water-borne paints with high volume solids based on bimodal latexes. *Progress in Organic Coatings*, 68(3), 225-233.
- Drake, I., Cardoen, G., Hughes, A., Nakatani, A. I., Landes, B., Reffner, J., & Even, R. (2019). Polyurea-acrylic hybrid emulsions: Characterization and film properties. *Polymer*, 181, Article#121761.
- Ebnesajjad, S. (2016). Introduction to plastics. In (pp. xiii-xxv): Elsevier.
- El-hoshoudy, A. N. M. B. (2018). Emulsion polymerization mechanism. *Recent Research in Polymerization*, Article#1, 3-14.
- El-Sherif, H., Nasser, A., Hussin, A., Abd El-Wahab, H., Ghazy, M., & Elsayed, A. (2017). Nano emulsion binders for paper coating synthesis and application. *Journal of Macromolecular Science, Part A*, 54(5), 271-287.
- El-Sherif, H., Nasser, A., Hussin, A., El-Wahab, A., Ghazy, M., & Elsayed, A. (2019). Tailoring of mechanical properties and printability of coated recycled papers. *Polymer Bulletin*, 76(6), 2965-2990.
- Erlangung, Z., & Nazaran, P. (2008). *Nucleation in Emulsion Polymerization Steps towards a Non-micellar Nucleation Theory*. PhD thesis, Potsdam University, Germany,
- Feldman, D. (2008). Polymer history. *Designed Monomers and Polymers*, 11(1), 1-15.
- Felton, L. A. (2013). Mechanisms of polymeric film formation. *International Journal of Pharmaceutics*, 457(2), 423-427.

- Francisco-Vieira, L., Benavides, R., Cuara-Diaz, E., & Morales-Acosta, D. (2019). Styrene-co-butyl acrylate copolymers with potential application as membranes in PEM fuel cell. *International Journal of Hydrogen Energy*, 44(24), 12492-12499.
- Germack, D. S., & Wooley, K. L. (2007). Isoprene polymerization via reversible addition fragmentation chain transfer polymerization. *Journal of Polymer Science Part A: Polymer Chemistry*, 45(17), 4100-4108.
- Gilbert, R. G. (1995). *Emulsion polymerization: a mechanistic approach*: Academic press.
- Gong, H., Gao, Y., Jiang, S., & Sun, F. (2018). Photocured materials with self-healing function through ionic interactions for flexible electronics. *ACS Applied Materials & Interfaces*, 10(31), 26694-26704.
- Gong, L., Liao, G., Luan, H., Chen, Q., Nie, X., Liu, D., & Feng, Y. (2020). Oil solubilization in sodium dodecylbenzenesulfonate micelles: New insights into surfactant enhanced oil recovery. *Journal of Colloid and Interface Science*, 569, 219-228.
- Govindaraju, S. V., Kulkarni, M. C., & Hui, M. K. S. (2018). Versatile new class of polymer for natural and synthetic rubber gloves coating.
- Harkins, W. D. (1945). A general theory of the reaction loci in emulsion polymerization. *The Journal of Chemical Physics*, 13(9), 381-382.
- Hua, H., & Dubé, M. A. (2011). Semi-continuous emulsion copolymerization of styrene-butyl acrylate with methacrylic acid: screening design of experiments. *Polymer-Plastics Technology and Engineering*, 50(4), 349-361.
- Ito, F., Ma, G., Nagai, M., & Omi, S. (2002). Study of particle growth by seeded emulsion polymerization accompanied by electrostatic coagulation. *Colloids and Surfaces A: Physicochemical and Engineering Aspects*, 201(1-3), 131-142.
- Iyer, V., Cayatte, C., Guzman, B., Schneider-Ohrum, K., Matuszak, R., Snell, A., Rajani, G. M., McCarthy, M. P., & Muralidhara, B. (2015). Impact of formulation and particle size on stability and immunogenicity of oil-in-water emulsion adjuvants. *Human Vaccines & Immunotherapeutics*, 11(7), 1853-1864.
- Jain, M., Vora, R., & Satpathy, U. (2003). Kinetics of emulsion copolymerization of methylmethacrylate and ethylacrylate: effect of type and concentration of initiator in unseeded polymerization system. *European Polymer Journal*, 39(10), 2069-2076.

- Janssen, R. (2006). Flexible coated article and method of making the same. In: Google Patents.
- Jauregui, D. (2016). Synthesis and Optimization of Emulsion Polymers.
- Jiaying, H., Jiayan, C., Jiaming, Z., Yihong, C., Lizong, D., & Yousi, Z. (2006). Some monomer reactivity ratios of styrene and (meth) acrylates in the presence of TEMPO. *Journal of Applied Polymer Science*, 100(5), 3531-3535.
- Jiao, C., Sun, L., Shao, Q., Song, J., Hu, Q., Naik, N., & Guo, Z. (2021). Advances in waterborne acrylic resins: Synthesis principle, modification strategies, and their applications. *ACS Omega*, 6(4), 2443-2449.
- Joseph, E., & Singhvi, G. (2019). Multifunctional nanocrystals for cancer therapy: a potential nanocarrier. *Nanomaterials for Drug Delivery and Therapy*, 91-116.
- Kamal, M. S., Hussein, I. A., & Sultan, A. S. (2017). Review on surfactant flooding: phase behavior, retention, IFT, and field applications. *Energy & Fuels*, 31(8), 7701-7720.
- Kieć-Świerczyńska, M., Świerczyńska-Machura, D., Chomiczewska-Skóra, D., Nowakowska-Świrta, E., & Kręcis, B. (2014). Occupational allergic and irritant contact dermatitis in workers exposed to polyurethane foam. *International Journal of Occupational Medicine and Environmental Health*, 27(2), 196-205.
- Kim, Y., Kwon, H. J., Kook, J.-W., Park, J. J., Lee, C., Koh, W.-G., Hwang, K.-S., & Lee, J.-Y. (2022). Wetting properties and morphological behavior of core-shell polymer-based nanoparticle coatings. *Progress in Organic Coatings*, 163, Article#106606.
- Kramer, A., & Assadian, O. (2016). Indications and the requirements for single-use medical gloves. *GMS Hygiene and Infection Control*, 11.
- Kumar, N. (2017). *Investigation on the effect of various cross-linking agents in acrylic emulsion polymer & its application performance* (Doctoral dissertation)
- Leiza, J. R., & Meuldijk, J. (2013). Emulsion copolymerisation, process strategies. *Chemistry and Technology of Emulsion Polymerisation*, 75-104.
- Lesage de la Haye, J., Martin-Fabiani, I., Schulz, M., Keddie, J. L., D'agosto, F., & Lansalot, M. (2017). Hydrophilic MacroRAFT-mediated emulsion polymerization: Synthesis of latexes for cross-linked and surfactant-free films. *Macromolecules*, 50(23), 9315-9328.

- Levison, M. (2009). Surfactant production: present realities and future perspectives. *Handbook of Detergents Part F: Production*, 142, 1-38.
- Li, P., Zhou, Z., Ma, W., & Hao, T. (2016). Core-shell emulsion polymerization of styrene and butyl acrylate in the presence of polymerizable emulsifier. *Journal of Applied Polymer Science*, 133(12).
- Liao, Y., Wang, Q., Xia, H., Xu, X., Baxter, S. M., Slone, R. V., Wu, S., Swift, G., & Westmoreland, D. G. (2001). Ultrasonically initiated emulsion polymerization of methyl methacrylate. *Journal of Polymer Science Part A: Polymer Chemistry*, 39(19), 3356-3364.
- Lin, Y., Ng, K. M., Chan, C.-M., Sun, G., & Wu, J. (2011). High-impact polystyrene/halloysite nanocomposites prepared by emulsion polymerization using sodium dodecyl sulfate as surfactant. *Journal of Colloid and Interface Science*, 358(2), 423-429.
- Lovell, P. A., & Schork, F. J. (2020). Fundamentals of emulsion polymerization. *Biomacromolecules*, 21(11), 4396-4441.
- Lu, G. W., & Gao, P. (2010). Emulsions and microemulsions for topical and transdermal drug delivery. In *Handbook of non-invasive drug delivery systems* (pp. 59-94): Elsevier.
- Lu, M., Keskkula, H., & Paul, D. (1996). Thermodynamics of solubilization of functional copolymers in the grafted shell of core-shell impact modifiers: 2. Experimental. *Polymer*, 37(1), 125-135.
- Lutz, H., Weitzel, H., & Huster, W. (2012). Aqueous Emulsion Polymers Wacker Chemie AG. *Burghausen, Germany*.
- Manhart, J., Hausberger, A., Maroh, B., Holzner, A., Schaller, R., Kern, W., & Schlögl, S. (2020). Tribological characteristics of medical gloves in contact with human skin and skin equivalents. *Polymer Testing*, 82, Article#106318.
- Mariz, I. d. F., de la Cal, J. C., & Leiza, J. R. (2011). Unimodal particle size distribution latexes: Effect of reaction conditions on viscosity and stability at high solids content. *Macromolecular Reaction Engineering*, 5(9-10), 361-372.
- Milovanovic, M., Arsenijevic, A., Milovanovic, J., Kanjevac, T., & Arsenijevic, N. (2017). Nanoparticles in antiviral therapy. In *Antimicrobial nanoarchitectonics* (pp. 383-410): Elsevier.



- Modha, S. H., Kister, M. E., & Huynh, L. V. (2005). Method of making a glove having improved donning characteristics. In: Google Patents.
- Mylon, P., Lewis, R., Carré, M. J., Martin, N., & Brown, S. (2014). A study of clinicians' views on medical gloves and their effect on manual performance. *American Journal of Infection Control*, 42(1), 48-54.
- Myre, E., & Shaw, R. (2006). The turbidity tube: simple and accurate measurement of turbidity in the field. *Michigan Technological University*.
- Nuzaimah, M., Sapuan, S., Nadlene, R., & Jawaid, M. (2021). Effect of surface treatment on the performance of polyester composite filled with waste glove rubber crumbs. *Waste and Biomass Valorization*, 12(2), 1061-1074.
- Odian, G. (2004). *Principles of polymerization*: John Wiley & Sons.
- Ong, E. (2001). *Recent advances in the Malaysia's glove industry in meeting today's healthcare challenges*. Paper presented at the Latex 2001 Conference Munich Germany.
- Ownby, D. R. (2002). A history of latex allergy. *Journal of Allergy and Clinical Immunology*, 110(2), S27-S32.
- Paulen, R., Benyahia, B., Latifi, M. A., & Fikar, M. (2013). Dynamic optimization of semi-batch emulsion co-polymerization reactor for styrene/butyl acrylate in the presence of a chain transfer agent. In *Computer Aided Chemical Engineering* (pp. 721-726): Elsevier.
- Pedro, R., & Walters, K. A. (2019). Surfactants in cosmetic products. *Cosmetic Formulation: Principles and Practice*, 129-162. CRC Press.
- Petrash, S., Xiao, C., Mukherjee, A., Li, Z., & Thomaides, J. S. (2004). Polymer coating for rubber articles. In: Google Patents.
- Pladis, P., & Kiparissides, C. (2014). Polymerization reactors.
- Preece, D., Hong Ng, T., Tong, H. K., Lewis, R., & Carré, M. J. (2021). The effects of chlorination, thickness, and moisture on glove donning efficiency. *Ergonomics*, 64(9), 1205-1216.
- Radabutra, S., Thanawan, S., & Amornsakchai, T. (2009). Chlorination and characterization of natural rubber and its adhesion to nitrile rubber. *European Polymer Journal*, 45(7), 2017-2022.

- Rahman, M. F. A., Rusli, A., & Azura, A. (2020). *Shelf life prediction of sago starch filled natural rubber latex gloves by using average activation energy approach*. Paper presented at the AIP Conference Proceedings.
- Ramos-Fernández, J. M., Beleña, I., Romero-Sánchez, M. D., Fuensanta, M., Guillem, C., & López-Buendía, Á. M. (2012). Study of the film formation and mechanical properties of the latexes obtained by miniemulsion co-polymerization of butyl acrylate, methyl acrylate and 3-methacryloxypropyltrimethoxysilane. *Progress in Organic Coatings*, 75(1-2), 86-91.
- Ren, Y., Zhang, Q., Yang, N., Xu, J., Liu, J., Yang, R., Kunkelmann, C., Schreiner, E., Holtze, C., & Mülheims, K. (2019). Molecular dynamics simulations of surfactant adsorption at oil/water interface under shear flow. *Particuology*, 44, 36-43.
- Ríos-Osuna, L. A., Licea-Claverie, A., Paraguay-Delgado, F., & Cortez-Lemus, N. A. (2016). Synthesis of poly (styrene-acrylates-acrylic acid) microspheres and their chemical composition towards colloidal crystal films. *International Journal of Polymer Science*, 2016.
- Roberts, A., & Brackley, C. (1996). Comfort and frictional properties of dental gloves. *Journal of Dentistry*, 24(5), 339-343.
- Saha, S., & Bhowmick, A. K. (2019). An Insight into molecular structure and properties of flexible amorphous polymers: A molecular dynamics simulation approach. *Journal of Applied Polymer Science*, 136(18), Article#47457.
- Sari, A. M., Suryani, A., Lotulung, P. D., & Tursiloadi, S. (2017). Preparation of alkyl halide as intermediate compound in synthesis cationic surfactant alkyl trimethyl ammonium chloride. *Jurnal Kimia Terapan Indonesia*, 19(1), 25-28.
- Sarkar, R., Pal, A., Rakshit, A., & Saha, B. (2021). Properties and applications of amphoteric surfactant: A concise review. *Journal of Surfactants and Detergents*, 24(5), 709-730.
- Selvamani, V. (2019). Stability studies on nanomaterials used in drugs. In *Characterization and biology of nanomaterials for drug delivery* (pp. 425-444): Elsevier.
- Sen, S., Mabuni, C., & Walsh, D. (2001). Development of a methodology for characterizing commercial chlorinated latex gloves. *Journal of Applied Polymer Science*, 82(3), 672-682.
- Shnoudeh, A. J., Hamad, I., Abdo, R. W., Qadumii, L., Jaber, A. Y., Surchi, H. S., & Alkelany, S. Z. (2019). Synthesis, characterization, and applications of metal nanoparticles. In *Biomaterials and bionanotechnology* (pp. 527-612): Elsevier.

- Songsiri, N., Rempel, G. L., & Prasassarakich, P. (2019). Isoprene synthesis using MIL-101 (Cr) encapsulated silicotungstic acid catalyst. *Catalysis Letters*, 149(9), 2468-2481.
- Sornsanee, P., Jitprarop, V., & Tangboriboon, N. (2018). *Preparation polyisoprene (NR) and polyacrylonitrile rubber latex glove films by dipping ceramic hand molds process and their properties*. Paper presented at the Defect and Diffusion Forum.
- Steward, P., Hearn, J., & Wilkinson, M. (2000). An overview of polymer latex film formation and properties. *Advances in Colloid and Interface Science*, 86(3), 195-267.
- Sun, H., & Wristers, J. (2000). Butadiene. *Kirk-Othmer Encyclopedia of Chemical Technology*.
- Tadros, T. F. (2013). *Emulsion formation and stability*: John Wiley & Sons.
- Tan, C., Tirri, T., & Wilen, C.-E. (2016). The effect of core-shell particle morphology on adhesive properties of poly (styrene-co-butyl acrylate). *International Journal of Adhesion and Adhesives*, 66, 104-113.
- Tauer, K. (2020). The role of emulsifiers in the kinetics and mechanisms of emulsion polymerization. In *Surfactants in Polymers, Coatings, Inks and Adhesives* (pp. 32-70): Blackwell.
- Thickett, S. C., & Gilbert, R. G. (2007). Emulsion polymerization: State of the art in kinetics and mechanisms. *Polymer*, 48(24), 6965-6991.
- Truscott, W. (2002). Glove powder reduction and alternative approaches. *Methods*, 27(1), 69-76.
- Tumnantong, D., Rempel, G. L., & Prasassarakich, P. (2017). Polyisoprene-silica nanoparticles synthesized via RAFT emulsifier-free emulsion polymerization using water-soluble initiators. *Polymers*, 9(11), Article#637.
- Van Herk, A., & Gilbert, R. (2013). Emulsion polymerisation. *Chemistry and Technology of Emulsion Polymerisation*, 43-73.
- Wang, X., Yang, K., Zong, C., & Zhang, P. (2021). The evolution of microstructure of Styrene-Isoprene-Butadiene Rubber during the thermal-oxidative aging process using In-situ FTIR way. *Polymer Degradation and Stability*, 188, Article#109573.

- Wichaita, W., Promlok, D., Sudjaipraparat, N., Sripraphot, S., Suteewong, T., & Tangboriboonrat, P. (2021). A concise review on design and control of structured natural rubber latex particles as engineering nanocomposites. *European Polymer Journal*, 159, Article#110740.
- Winnik, M. A. (1997). Latex film formation. *Current Opinion in Colloid & Interface Science*, 2(2), 192-199.
- Yamak, H. B. (2013). Emulsion polymerization: effects of polymerization variables on the properties of vinyl acetate based emulsion polymers. In *Polymer Science: IntechOpen*.
- Yeh, Y.-S. T. (2002). Powder-free gloves having a coating containing cross-linked polyurethane and silicone and method of making the same. In: Google Patents.
- Yeh, Y.-S. T., & Zhu, D. (2002). Powder-free nitrile-coated gloves with an intermediate rubber-nitrile layer between the glove and the coating and method of making same. In: Google Patents.
- Yekeen, N., Padmanabhan, E., Syed, A. H., Sevoo, T., & Kanesen, K. (2020). Synergistic influence of nanoparticles and surfactants on interfacial tension reduction, wettability alteration and stabilization of oil-in-water emulsion. *Journal of Petroleum Science and Engineering*, 186, Article#106779.
- Yew, G. Y., Tham, T. C., Law, C. L., Chu, D.-T., Ogino, C., & Show, P. L. (2019). Emerging crosslinking techniques for glove manufacturers with improved nitrile glove properties and reduced allergic risks. *Materials Today Communications*, 19, 39-50.
- Yip, E., & Cacioli, P. (2002). The manufacture of gloves from natural rubber latex. *Journal of Allergy and Clinical Immunology*, 110(2), S3-S14.
- Zhang, C. Y., Zhu, Z. W., & Gong, S. L. (2017). Synthesis of stable high hydroxyl content self-emulsifying waterborne polyacrylate emulsion. *Journal of Applied Polymer Science*, 134(21).
- Zhang, H. (2016). Surface characterization techniques for polyurethane biomaterials. In *Advances in polyurethane biomaterials* (pp. 23-73): Elsevier.
- Zhong, Z., Yu, Q., Yao, H., Wu, W., Feng, W., Yu, L., & Xu, Z. (2013). Study of the styrene-acrylic emulsion modified by hydroxyl-phosphate ester and its stoving varnish. *Progress in Organic Coatings*, 76(5), 858-862.

Zubitur, M., & Asua, J. (2001). Factors affecting kinetics and coagulum formation during the emulsion copolymerization of styrene/butyl acrylate. *Polymer*, 42(14), 5979-5985.

Universiti Malaya